Part 5: Atomization, Drop Breakup/Coalescence

Reciprocating Internal Combustion Engines

Prof. Rolf D. Reitz
Engine Research Center
University of Wisconsin-Madison

2014 Princeton-CEFRC
Summer School on Combustion
Course Length: 15 hrs

(Mon.- Fri., June 23 – 27, 2014)

Short course outine:

Engine fundamentals and performance metrics, computer modeling supported by in-depth understanding of fundamental engine processes and detailed experiments in engine design optimization.

Day 1 (Engine fundamentals)
- Part 1: IC Engine Review, 0, 1 and 3-D modeling
- Part 2: Turbochargers, Engine Performance Metrics

Day 2 (Combustion Modeling)
- Part 3: Chemical Kinetics, HCCI & SI Combustion
- Part 4: Heat transfer, NOx and Soot Emissions

Day 3 (Spray Modeling)
- Part 5: Atomization, Drop Breakup/Coalescence
- Part 6: Drop Drag/Wall Impinge/Vaporization/Sprays

Day 4 (Engine Optimization)
- Part 7: Diesel combustion and SI knock modeling
- Part 8: Optimization and Low Temperature Combustion

Day 5 (Applications and the Future)
- Part 9: Fuels, After-treatment and Controls
- Part 10: Vehicle Applications, Future of IC Engines

Resolution – predictive models

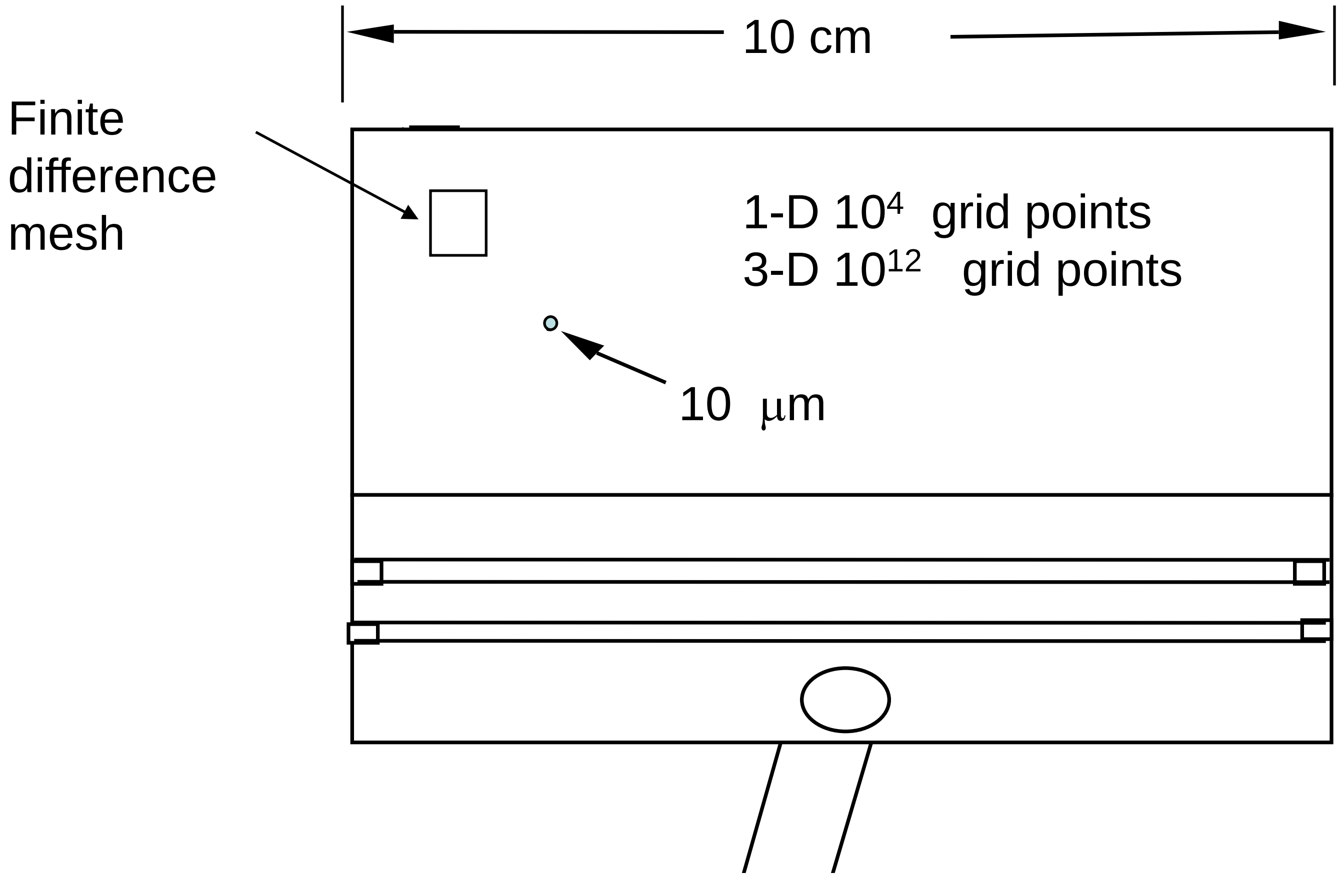

Models will not be entirely predictive for decades
Accurate submodels will be needed for detailed spray processes
(e.g., drop drag, drop turbulence interaction, vaporization, atomization, drop breakup, collision and coalescence, and spray/wall interaction)

Amsden,1997

Governing Equations

Gas phase

Liquid phase

Turbulence

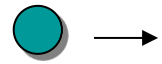

$\mathbf{x}, \mathbf{v}, r, Td$

$$f = f(\mathbf{x}, \mathbf{v}, \mathrm{r}, \mathrm{T_d}; \mathrm{t})$$

Gas void fraction and drop number density

Lagrangian Drop,
Eulerian Fluid (LDEF) models

$$\theta = 1 - \int_{Vol} \left(\iiint \frac{4}{3}\pi r^3 f \, dr \, d\mathbf{v} \, dT_d \right) dVol / Vol$$

Two-Phase Flow Regimes

Current LDEF spray models:
– drops occupy no volume θ >0.9

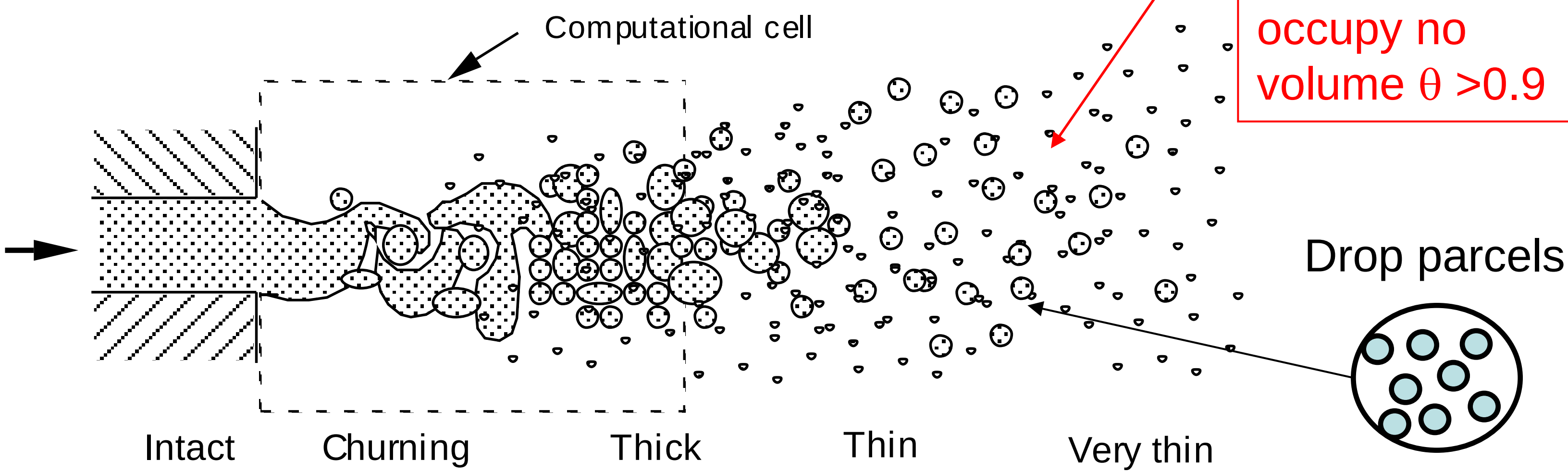

Dukowicz, 1980

LDEF Spray Modeling

- Concept of using “drop parcels”

  For typical heavy-duty diesel, injected fuel per cycle (75% load): 0.160 g

  One spray plume: m_{fuel}=0.160/6=0.0267 g

  If average SMD=10 μm → m_{drop} =3.8×10^{-10} g

  # of drops in the domain=0.0267g/m_{drop}=7.1×10^{7}

  Impractical to track individual fuel drops – group identical drops into ‘parcels’

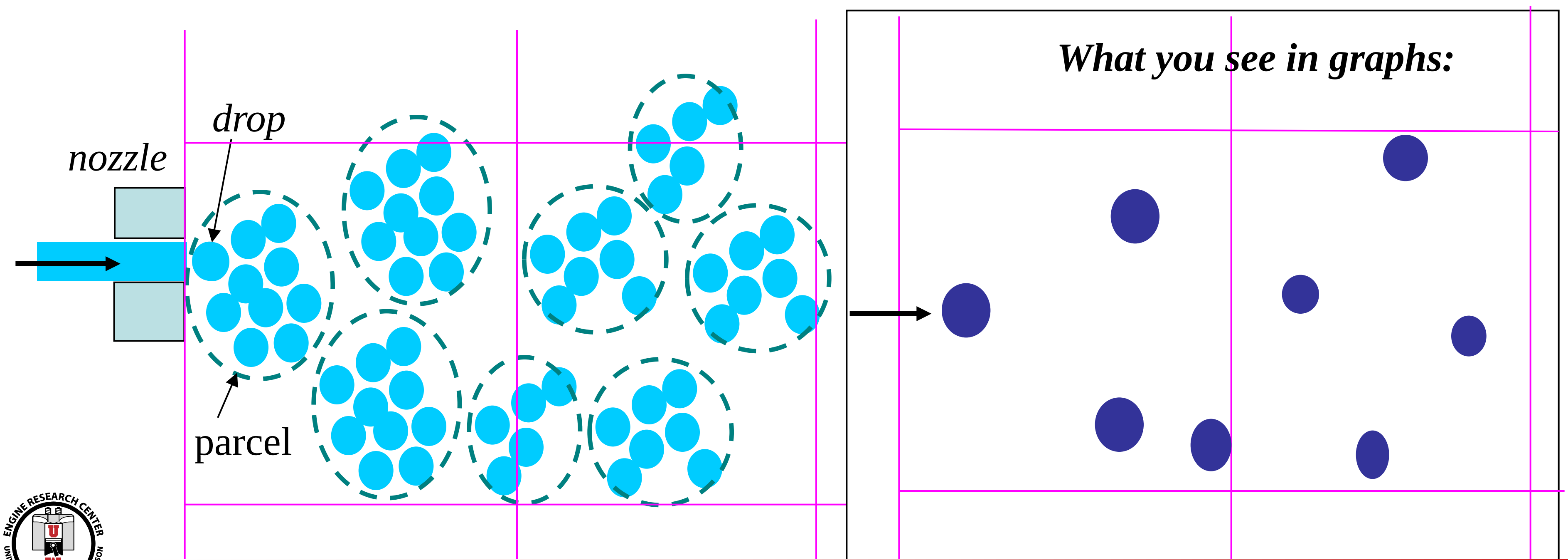

Amsden,1997

Eulerian Gas Phase

Mass conservation (species)

$$\frac{\partial \rho}{\partial t} + \nabla \cdot (\rho \mathbf{u}) = -\iiint \rho_l 4\pi r^2 R f \, dr d\mathbf{v} \, dT_d$$

$R = dr/dt$ - Vapor source

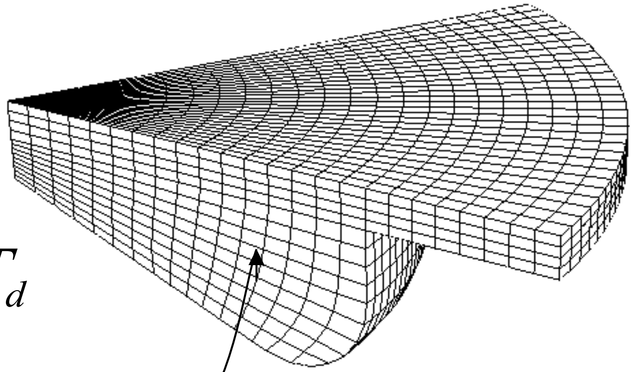

Momentum conservation

$$\frac{\partial \rho \mathbf{u}}{\partial t} + \nabla \cdot (\rho \mathbf{u} \mathbf{u}) = -\nabla p - \nabla(\tfrac{2}{3} \rho k) + \nabla \boldsymbol{\tau} + F^s + \rho \mathbf{g}$$

Turbulent and viscous stress

Rate of momentum gain due to spray – drop drag

Amsden,1989

Gas Phase (2)

Internal energy conservation

$$\frac{\partial \rho I}{\partial t} + \nabla \cdot (\rho \mathbf{u} I) = -P \nabla \cdot \mathbf{u} - \nabla \cdot \mathbf{J} + \rho \varepsilon + Q^c + Q^s$$

Combustion heat release (Q^c)

Turbulence dissipation ($\rho\varepsilon$)

Energy due to Spray - vaporization (Q^s)

Heat flux

$$\mathbf{J} = -\lambda \nabla T - \rho D \sum_m h_m \nabla(\rho_m / \rho)$$

Equations of state

$$p = RT \sum_m \rho_m / W_m$$

Specific heat, enthalpy from JANAF data

Liquid Phase

Spray drop number conservation $f = f\,(\mathbf{x}, \mathbf{v}, r, T_d, y, \dot{y}; t)$

$$\frac{\partial f}{\partial t} + \nabla_{\mathbf{x}} \cdot (f\mathbf{v}) + \nabla_{\mathbf{v}} \cdot (f\mathbf{F}) + \frac{\partial}{\partial r}(fR) + \frac{\partial}{\partial T_d}(f\dot{T}_d) + \frac{\partial}{\partial y}(f y) + \frac{\partial}{\partial y}(f\dot{y}) = \dot{f}_{coll} + \dot{f}_{bu}$$

$\boldsymbol{F} = d\mathbf{v}/dt$
drop drag

$R = dr/dt$
Vaporization and heating

Drop distortion

Drop breakup, coalescence

Spray exchange functions

$$\mathbf{F}^s = -\int f\rho_d \left(4/3\,\pi r^3 \mathbf{F}' + 4\pi r^2 R\mathbf{v}\right) d\mathbf{v}\; dr\; dT_d\; dy\; dy$$

$$\mathbf{Q}^s = -\int f\rho_d \left\{4\pi r^2 R\left[I_l + \tfrac{1}{2}(\mathbf{v}-\mathbf{u})^2\right] + 4/3\,\pi r^3\left[c_l T_d + \mathbf{F}'\cdot(\mathbf{v}-\mathbf{u}-\mathbf{u}')\right]\right\} d\mathbf{v}\; dr\; dT_d\; dy\; dy$$

Work done by drop drag forces $W^s = -\int f\rho_d\, 4/3\,\pi r^3 \mathbf{F}'\cdot\mathbf{u}'\; d\mathbf{v}\; dr\; dT_d\; dy\; dy$

Amsden, 1997

Lagrangian drop - liquid phase

Discrete Drop Model

drop position

$$\frac{d\mathbf{x}}{dt} = \mathbf{v}$$

drop velocity

$$\frac{d\mathbf{v}}{dt} = \mathbf{F}$$

drop size

$$\frac{d\mathrm{r}}{dt} = \mathbf{R}$$

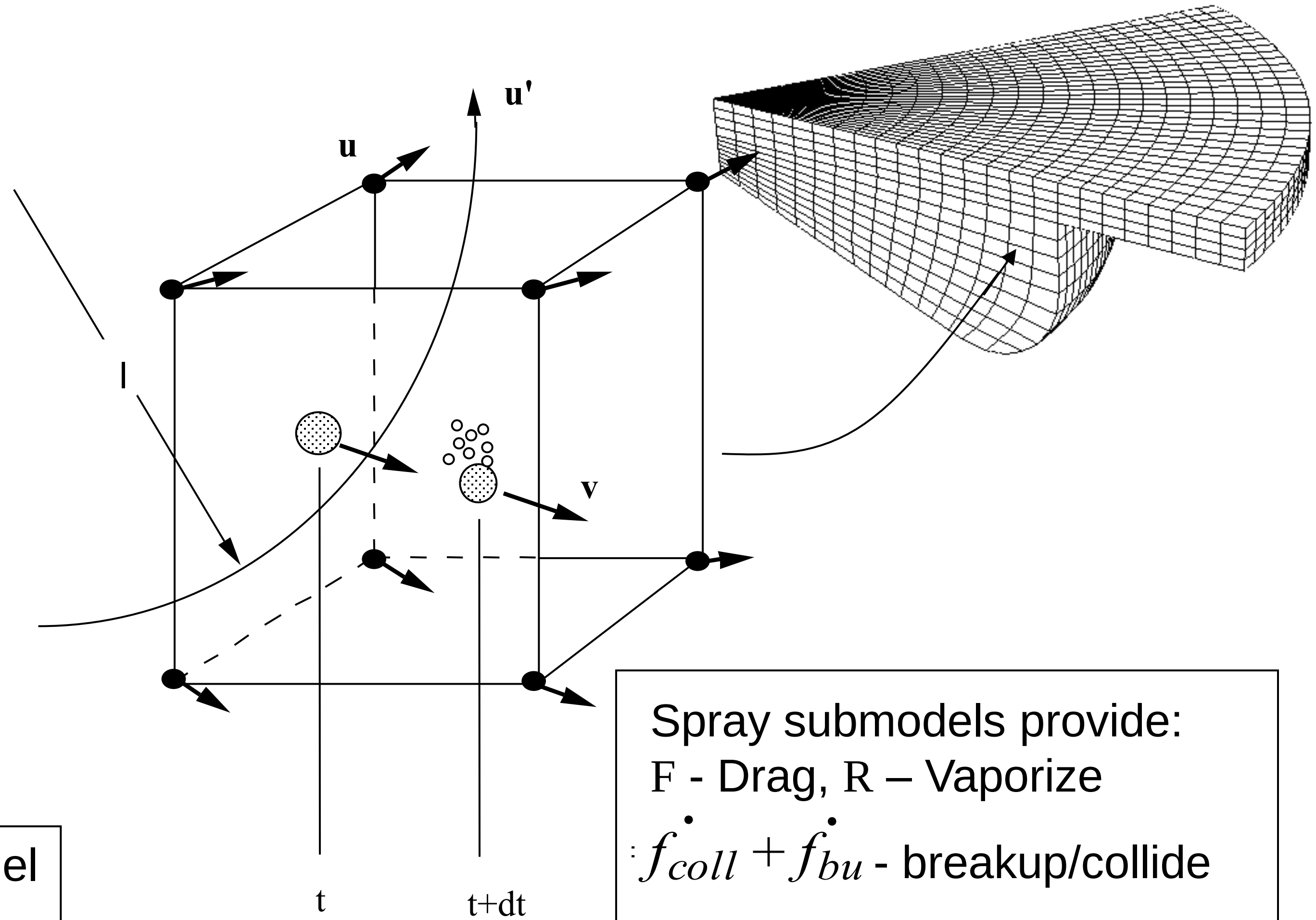

Turbulence model provides: l, $\boldsymbol{u}'$

Spray submodels provide:
F - Drag, R – Vaporize
$\dot{f}_{coll} + \dot{f}_{bu}$ - breakup/collide

Initial data:
v, *r*, T_d – Atomization model

Amsden, 1997

Turbulence Model (RANS)

Kinetic energy

$$\frac{\partial \rho k}{\partial t} + \nabla \cdot (\rho \mathbf{u} k) = -\tfrac{2}{3}\rho k \nabla \cdot \mathbf{u} + \underbrace{\boldsymbol{\tau} : \nabla \mathbf{u}}_{\text{Production due to mean flow}} + \nabla \cdot \left[\left(\frac{\mu}{\mathrm{Pr}_k}\right) \nabla k \right] \overbrace{- \rho \varepsilon}^{\text{Dissipation}} + \underbrace{\dot{W}^s}_{\text{Rate of work to disperse drops}}$$

Dissipation

Production due to mean flow

Rate of work to disperse drops

Dissipation rate

$$\frac{\partial \rho \varepsilon}{\partial t} + \nabla \cdot (\rho \mathbf{u} \varepsilon) = -\left(\frac{2}{3} C_{\varepsilon 1} - C_{\varepsilon 3}\right) \rho \varepsilon \nabla \cdot \mathbf{u} + \nabla \cdot \left[\left(\frac{\mu}{\mathrm{Pr}_\varepsilon}\right) \nabla \varepsilon \right] + \frac{\varepsilon}{k} \left[C_{\varepsilon 1} \boldsymbol{\tau} : \nabla \mathbf{u} - C_{\varepsilon 2} \rho \varepsilon + C_s \dot{W}^s \right]$$

Turbulence diffusivity

$$D = C_\mu k^2 / \varepsilon$$

Eddy size

$$l = C k^{3/2} / \varepsilon$$

Turbulence intensity

$$u'^2 = (2k/3)$$

UW-ERC Multidimensional CFD models

Submodel	Los Alamos	UW-Updated	References
intake flow	assumed initial flow	compute intake flow	SAE 951200
heat transfer	law-of-the-wall	compressible, unsteady	SAE 960633
turbulence	standard k-ε	RNG k-ε /LES	CST 106, 1995
nozzle flow	none	cavitation modeling	SAE 1999-01-0912
atomization	Taylor Analogy	surface-wave-growth	SAE 960633
		Kelvin Hemholtz	SAE 980131
		Rayleigh Taylor	CST 171, 1998
drop breakup	Taylor Analogy	Rayleigh Taylor	Atom. Sprays 1996
drop drag	rigid sphere	drop distortion	SAE 960861
wall impinge	none	rebound-slide model	SAE 880107
		wall film/splash	SAE 982584
collision/coalesce	O'Rourke	shattering collisions	Atom. Sprays 1999
vaporization	single component	multicomponent fuels	SAE 2000-01-0269
	low pressure	high pressure	SAE 2001-01-0998
ignition	Arrhenius	reduced chemistry	SAE 2004-01-0558
combustion	Arrhenius	CTC/GAMUT	SAE 2004-01-0102
		reduced kinetics	SAE 2003-01-1087
NOx	Zeldo'vich	Extended Zeldo'vich	SAE 940523
soot	none	Hiroyasu & Surovkin	SAE 960633
		Nagle Strickland oxidation	SAE 980549

Reitz, 1982

Atomization models (Single hole nozzle)

Four main jet breakup regimes:
Rayleigh, first wind-induced, second wind-induced and atomization

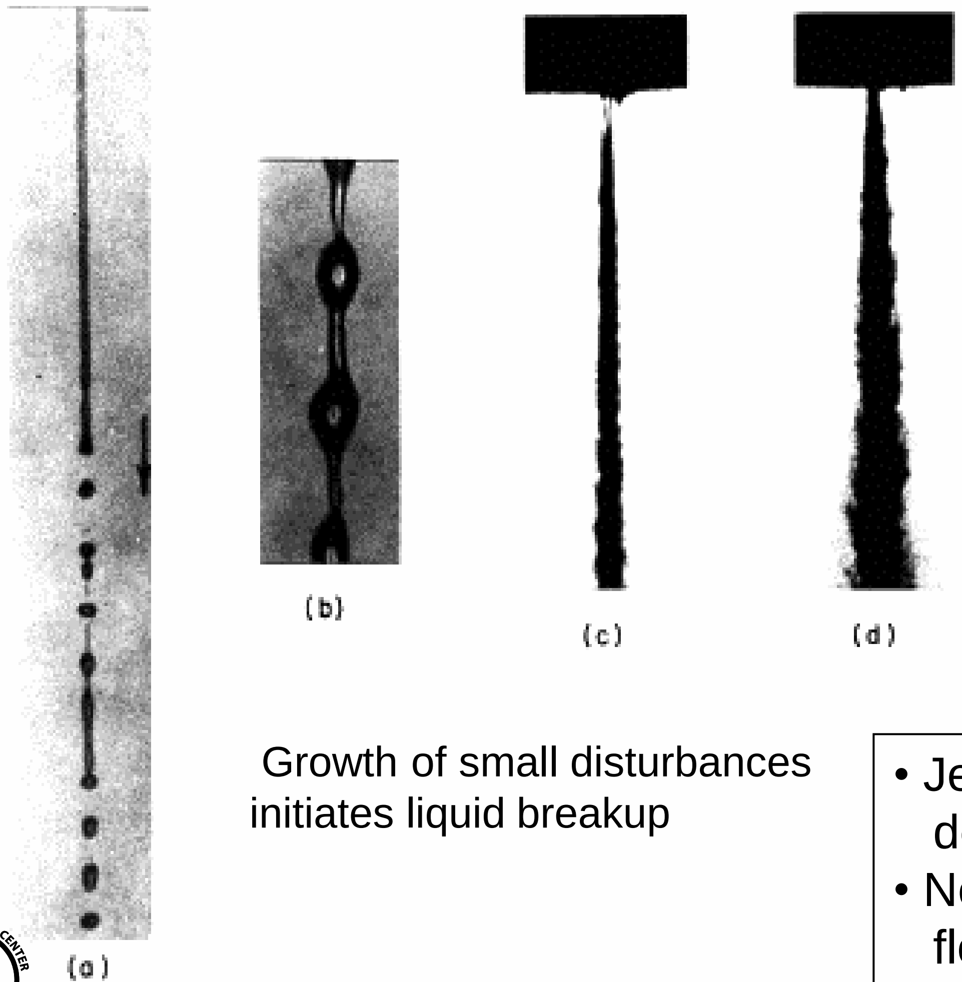

a.) Rayleigh breakup
Drop diameters > jet diameter.
Breakup far downstream nozzle

b.) First wind-induced regime
Drop diameter ~ jet diameter.
Breakup far downstream of nozzle

c.) Second wind-induced regime
Drop sizes < jet diameter.
Breakup starts close to nozzle exit

d.) Atomization regime
Drop sizes << jet diameter.
Breakup at nozzle exit.

Growth of small disturbances initiates liquid breakup

- Jet breakup known to depend on nozzle design details.
- Need to start by considering flow in the injector nozzle passage

Sarre, 1999

Cavitation inception

Account for effects of nozzle geometry

Cavitation if $P < P_V$

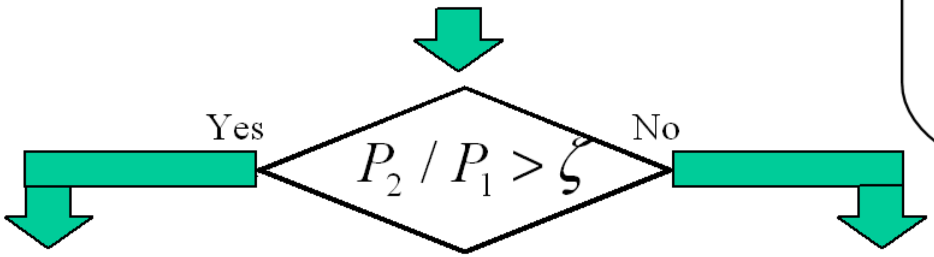

Cavitating flow

Non-cavitating flow

$$\zeta = \frac{1}{2(C_c - C_c^2)}$$

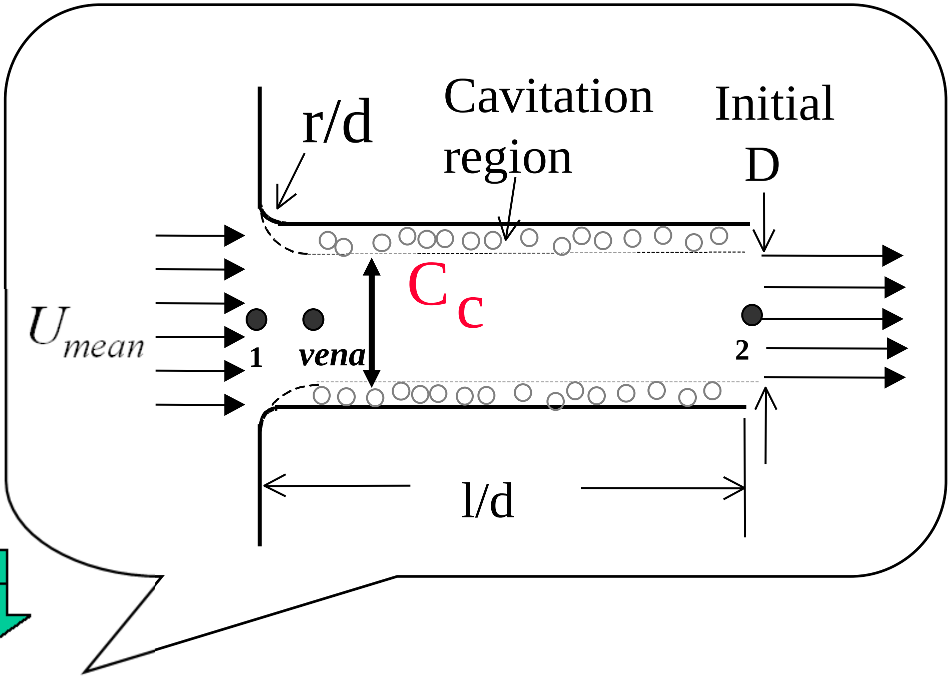

Contraction coefficient (Nurick (1976))

$$C_c = [(\frac{1}{0.62})^2 - 11.4 r/d]^{-1/2}$$

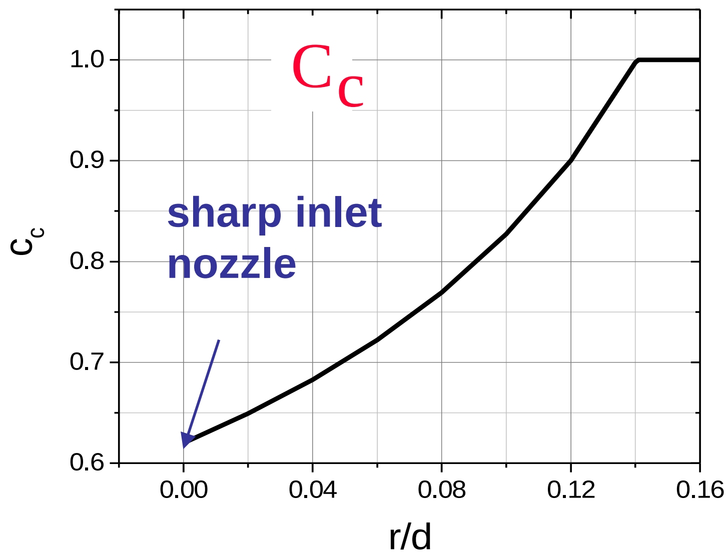

Sarre, 1999

ERC Nozzle Flow Model

$$P_2 / P_1 > \zeta$$

Cavitating flow (Yes)

Nozzle discharge coefficient

$$C_d = C_c \sqrt{\frac{p_1 - p_v}{p_1 - p_2}}$$

Effective injection velocity

$$u_{eff} = \frac{2C_c P_1 - P_2 + (1 - 2C_c) P_v}{C_c \sqrt{2\rho (P_1 - P_v)}}$$

Effective nozzle area

$$A_{eff} = \frac{2C_c^2 (P_1 - P_v)}{2C_c P_1 - P_2 + (1 - 2C_c) P_v} A$$

Non-cavitating flow (No)

Nozzle discharge coefficient

Lichtarowicz (1965)

$$C_d = 0.827 - 0.0085 \, {}^{l}\!/_{d}$$

Effective injection velocity

$$u_{eff} = C_d \sqrt{\frac{2(P_1 - P_2)}{\rho}}$$

Effective nozzle area

$$A_{eff} = A$$

Lee, 2010

Nozzle flow - cavitation

Homogeneous Equilibrium Model
- single phase mixture of vapor and liquid
- considers variable compressibility of mixture.

(1) Sonic Speed of mixture
: function of void fraction

$$\alpha = \frac{\rho_l - \rho}{\rho_l - \rho_v}$$

α=0 for pure liquid
α=1 for pure vapor

$$\frac{1}{a^2} = \left[\alpha\rho_v + (1-\alpha)\rho_l\right]\left[\frac{\alpha}{\rho_v a_v^2} + \frac{1-\alpha}{\rho_l a_l^2}\right]$$

(Wallis, 1967)

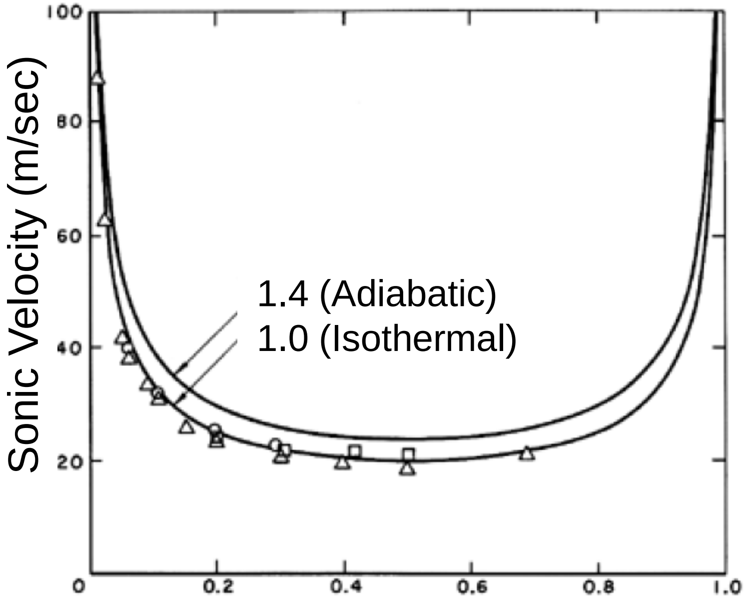

Sonic velocity in bubbly air/water mixture at atmospheric pressure
Brennen (1995)

(2) Equation of State of mixture

: by integrating $dP = a^2 d\rho$ (Schmidt, 1997)

$$P = P_l^{sat} + P_{vl}\log\left[\frac{\rho_v a_v^2\left(\rho_l + \alpha(\rho_v - \rho_l)\right)}{\rho_l\left(\rho_v a_v^2 - \alpha\left(\rho_v a_v^2 - \rho_l a_l^2\right)\right)}\right]$$

$$P_{vl} = \frac{\rho_v a_v^2 \rho_l a_l^2 (\rho_v - \rho_l)}{\rho_v^2 a_v^2 - \rho_l^2 a_l^2} \qquad P_l^{sat} = P_v^{sat} + P_{vl}\log\left[\frac{\rho_v^2 a_v^2}{\rho_l^2 a_l^2}\right]$$

Lee, 2010

Nozzle flow - cavitation

max velocity at exit, cm/s

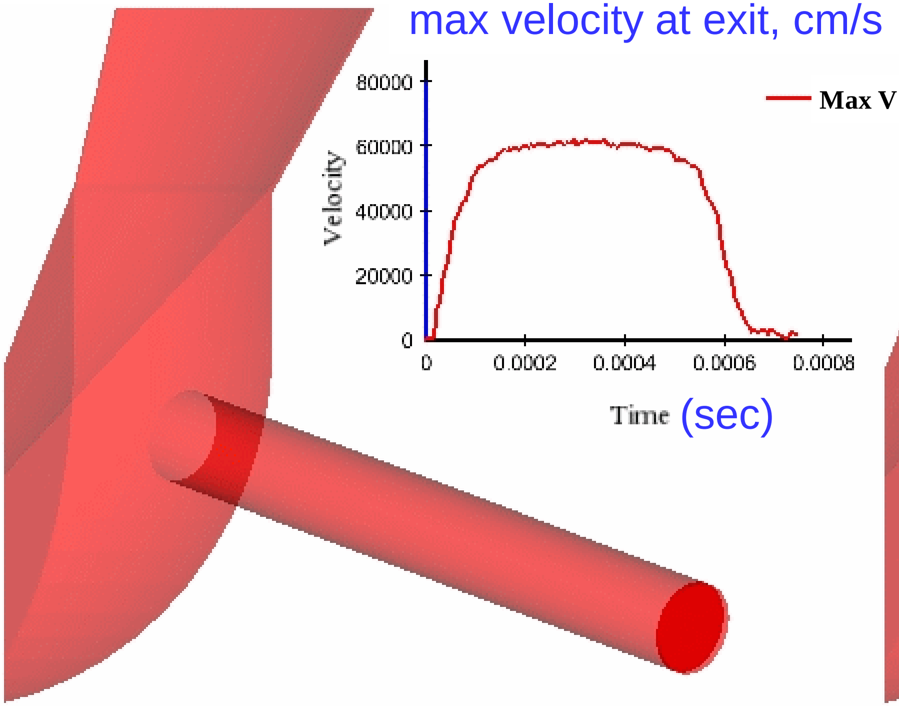

Time (sec)

min. density at exit, g/cm^3

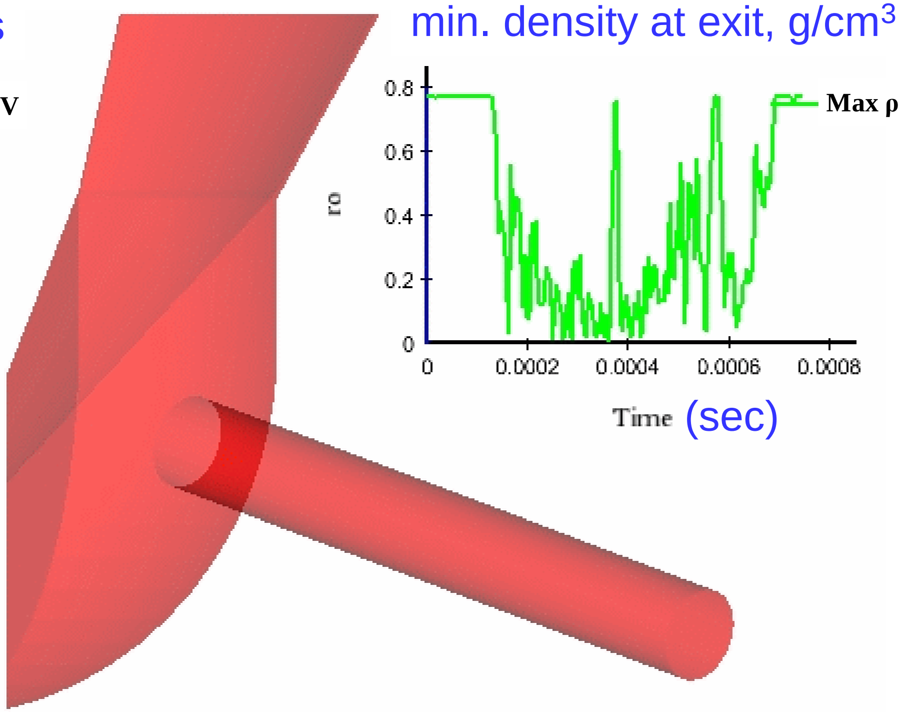

Time (sec)

streamline and exit velocity

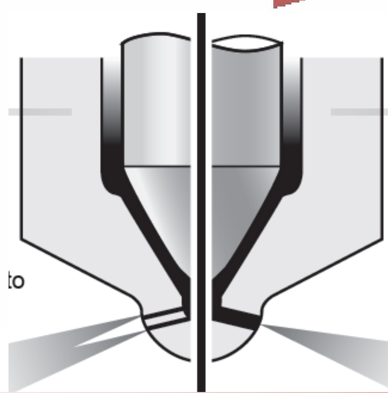

density and iso-surface (ρ=0.35g/cm^3)

ro
7.000e-001
5.250e-001
3.500e-001
1.750e-001
0.000e+000

Wang,, 2014

Eulerian flow models

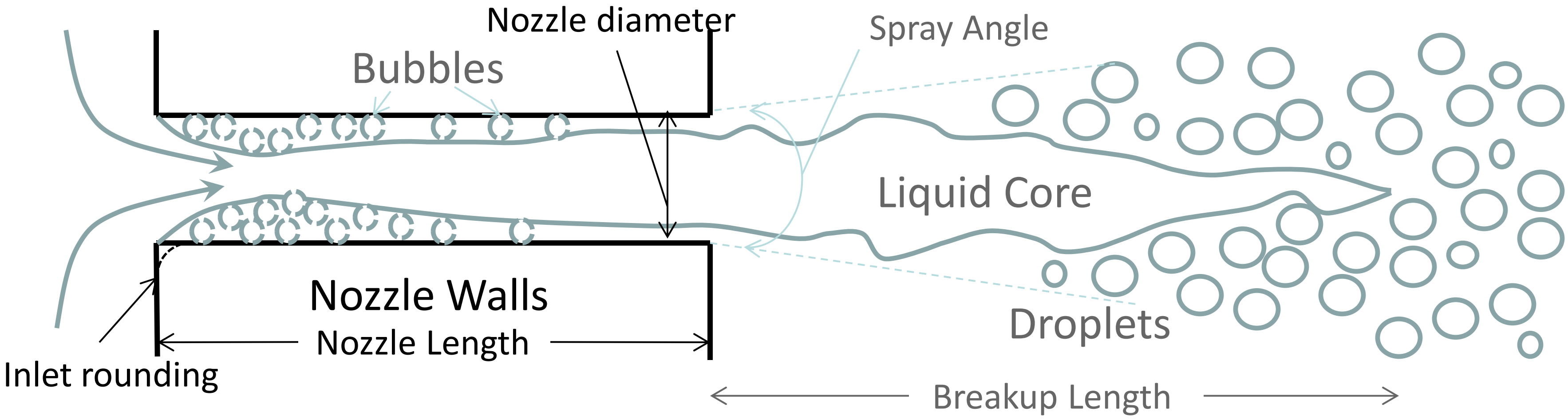

Develop a CFD Model that:

1) Simulates internal nozzle flow and external sprays simultaneously;

2) Models the thermodynamic states of the compressible liquid and gas;

3) Is able to simulate flows with large pressure and density ratios (1000:1);

4) Predicts phase change based on the 2nd Law of Thermodynamics;

5) Offers the capability of Eulerian-Lagrangian transition for dispersed sprays; (Eulerian-Lagrangian Spray and Atomization (ELSA) Model)

6) Models the sub-grid liquid-gas interface area density for the ELSA Model.

7-Equation model - Eulerian Fluid Solver

Relaxation terms

Gas

$$\frac{\partial \alpha_g \rho_g}{\partial t} + \nabla \cdot \left[\alpha_g \rho_g \mathbf{u}\right] = 0 \qquad (1)$$

$$\frac{\partial \alpha_g \rho_g \mathbf{u}_g}{\partial t} + \nabla \cdot \left[\alpha_g \rho_g \mathbf{u}_g \otimes \mathbf{u}_g\right] + \nabla \alpha_g p_g = P_I \nabla \alpha_g + \lambda\left(\mathbf{u}_l - \mathbf{u}_g\right) \qquad (2)$$

$$\frac{\partial \alpha_g E_g}{\partial t} + \nabla \cdot \left[\alpha_g \left(E_g + p_g\right)\mathbf{u}_g\right] = P_I \mathbf{u}_I \cdot \nabla \alpha_g + \lambda \mathbf{u}_I \cdot \left(\mathbf{u}_l - \mathbf{u}_g\right) + \mu P_I \left(p_l - p_g\right) \qquad (3)$$

Liquid

$$\frac{\partial \alpha_l \rho_l}{\partial t} + \nabla \cdot \left[\alpha_l \rho_l \mathbf{u}\right] = 0 \qquad (4)$$

$$\frac{\partial \alpha_l \rho_l \mathbf{u}_l}{\partial t} + \nabla \cdot \left[\alpha_l \rho_l \mathbf{u}_l \otimes \mathbf{u}_l\right] + \nabla \alpha_l p_l = P_I \nabla \alpha_l - \lambda\left(\mathbf{u}_l - \mathbf{u}_g\right) \qquad (5)$$

$$\frac{\partial \alpha_l E_l}{\partial t} + \nabla \cdot \left[\alpha_l \left(E_l + p_l\right)\mathbf{u}_l\right] = P_I \mathbf{u}_I \cdot \nabla \alpha_l - \lambda \mathbf{u}_I \cdot \left(\mathbf{u}_l - \mathbf{u}_g\right) - \mu P_I \left(p_l - p_g\right) \qquad (6)$$

$$\frac{\partial \alpha_g}{\partial t} + \mathbf{u} \cdot \nabla \alpha_g = \mu\left(p_l - p_g\right) \qquad (7)$$

Stiffened Gas Equation of State:

$$p_g = \left(\gamma_g - 1\right)\rho_g\left(e_g - q_g\right) - \gamma_g \pi_g$$

$$p_l = \left(\gamma_l - 1\right)\rho_l\left(e_l - q_l\right) - \gamma_l \pi_l$$

Liquid-Vapor-Air 3-phase mixture

CFD Approach

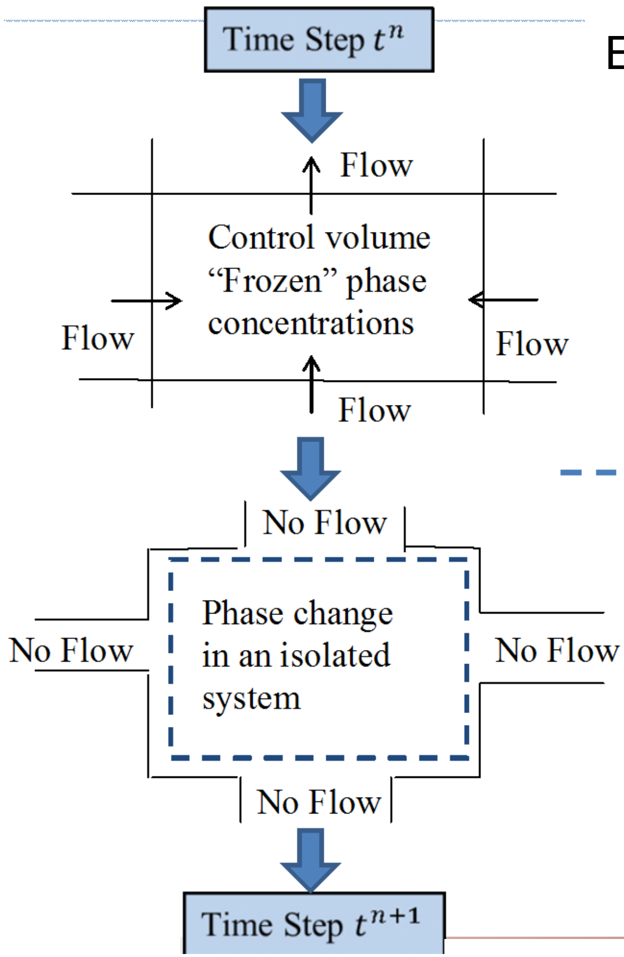

Equations solved with hybrid Rusanov HLLC scheme

Step 1: Solve Fluid Mechanics

- Eulerian compressible two-fluid approach
- Stiffened gas equation of state
- Assume “frozen” phase concentrations

Step 2: Solve Phase Equilibrium

- Assume static flow field
- Control volume treated as isolated thermodynamic system
- From the 2nd Law of Thermodynamics, use Entropy Maximization Principle to compute equilibrium phase compositions

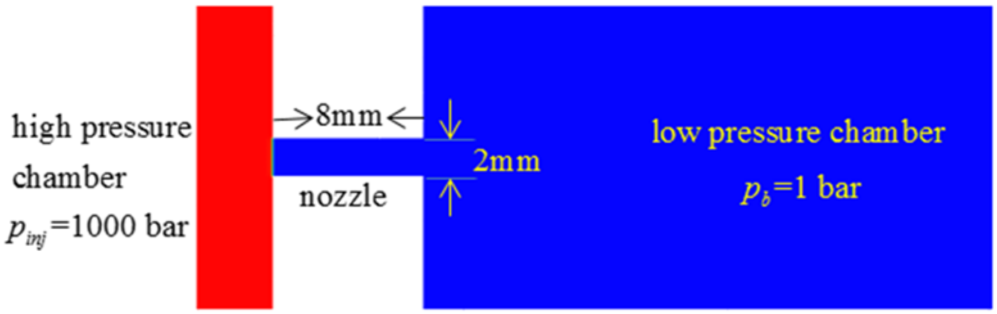

Wang,, 2014

Submerged Liquid Jet

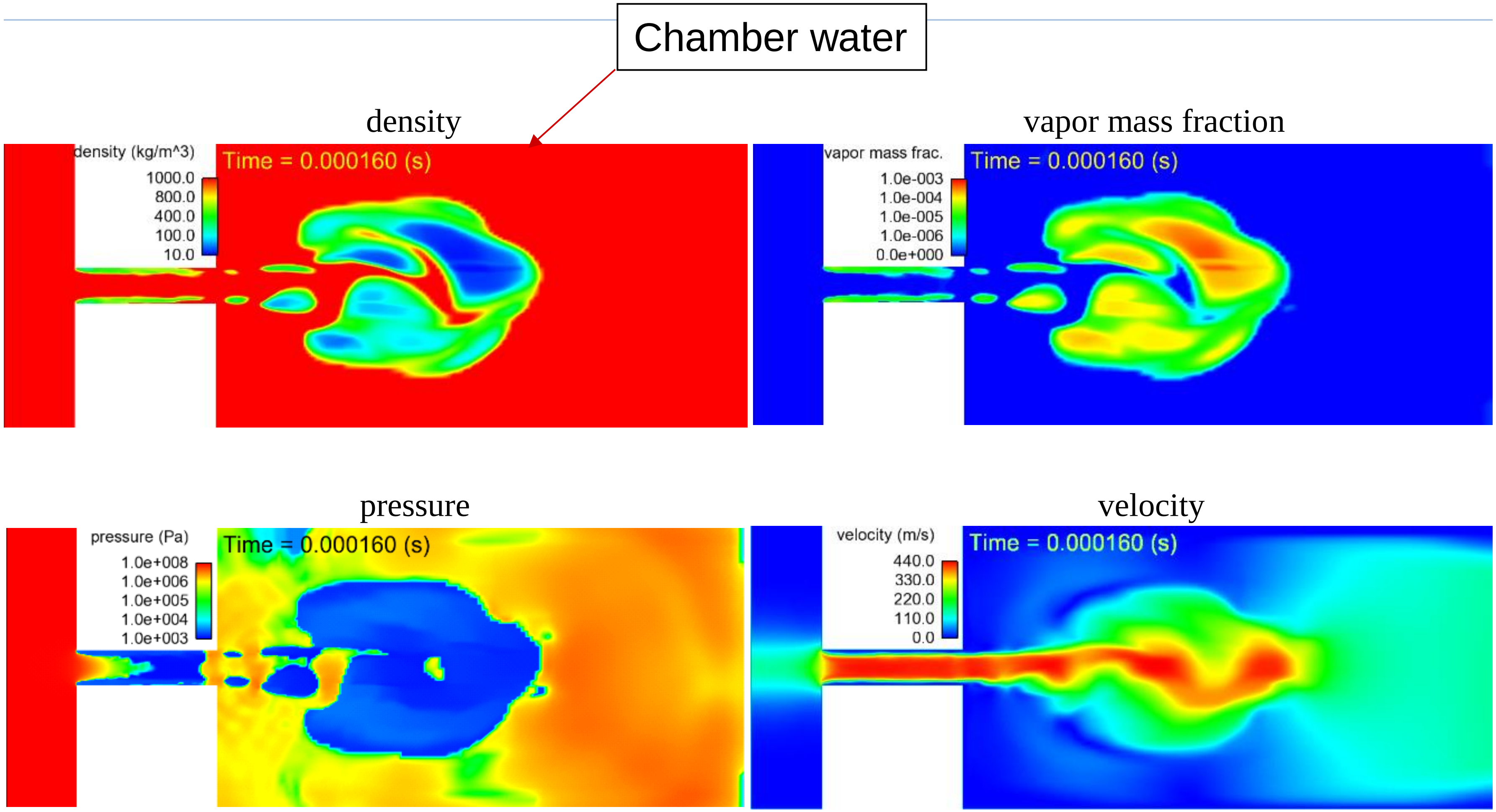

Water injected into water:
Cavitation is generated over entire length of nozzle walls.
Large region of cavitated fluid (bubble cloud) appears in chamber.

Submerged Liquid Jet

Chamber water

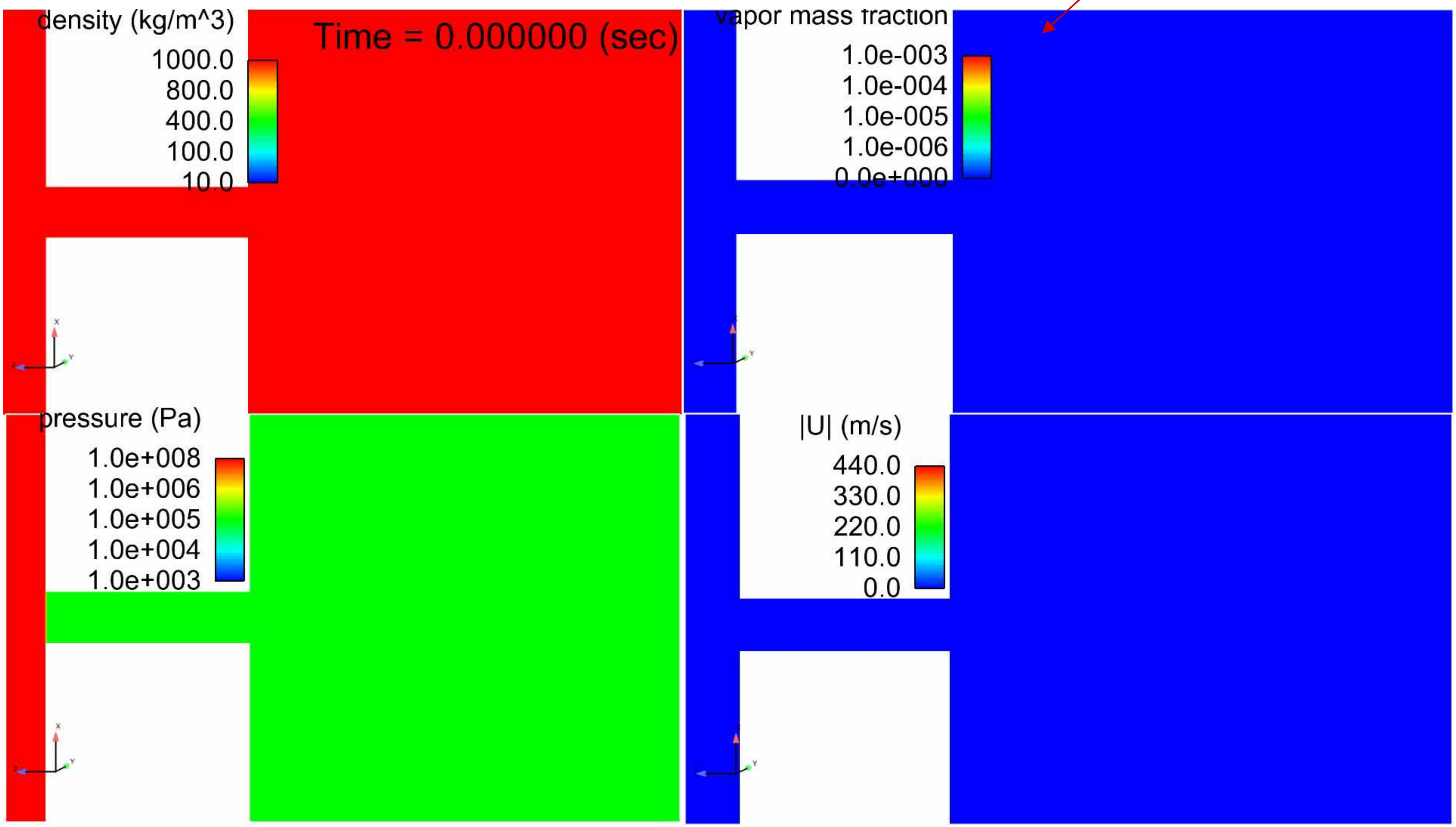

Water injected into water:
Cavitation generated over portions of nozzle passage.
Large region of cavitated fluid (bubble cloud) appears in chamber.

Part 5: Atomization, Drop Breakup/Coalescence

Wang,, 2014

Cavitating Liquid Jet

Non-condensible air

density

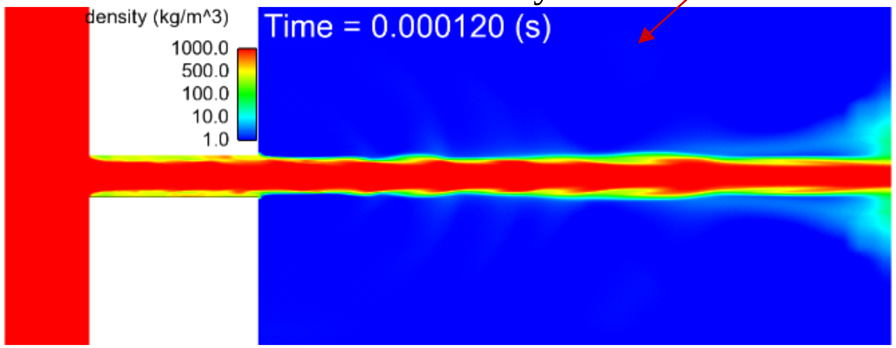

vapor mass fraction

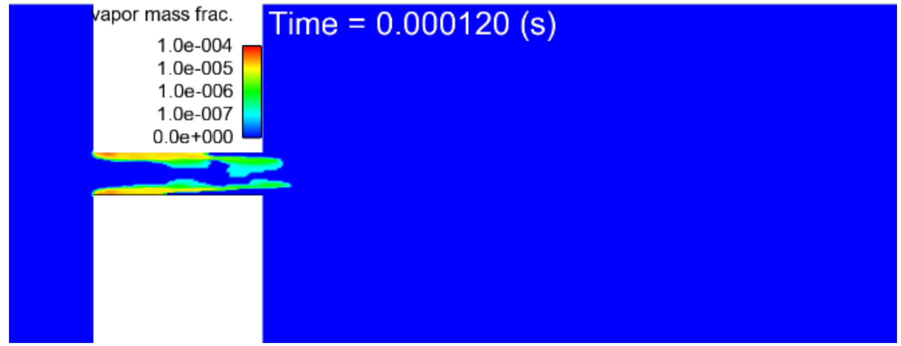

pressure

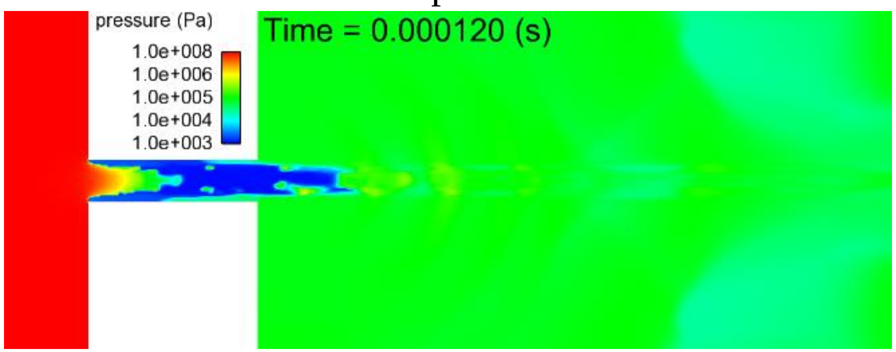

velocity

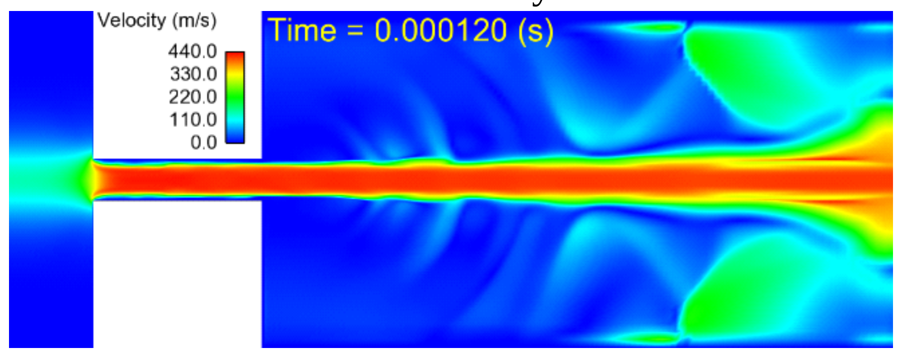

Air mass fraction

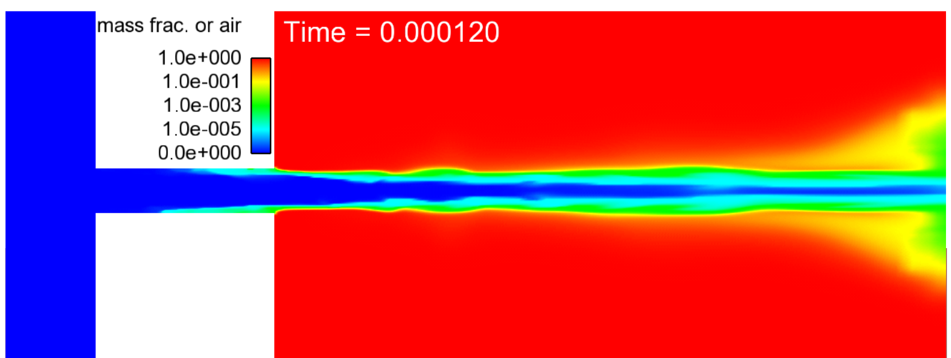

Low pressure (vapor pressure) regions seen within entire nozzle

Wang,, 2014

Cavitating Liquid Jet

Non-condensible air

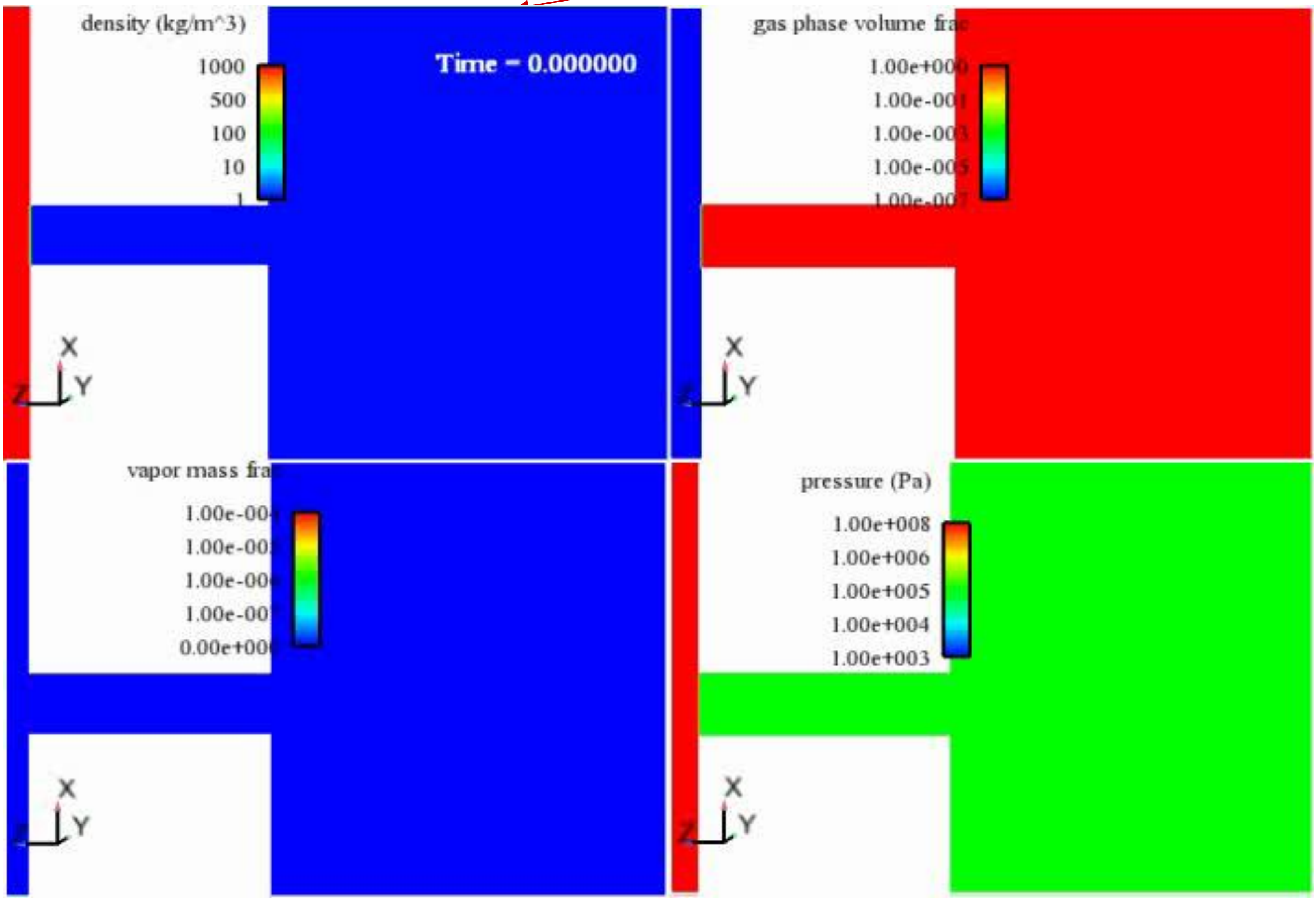

Reitz, 1982

Atomization - “Wave” breakup model

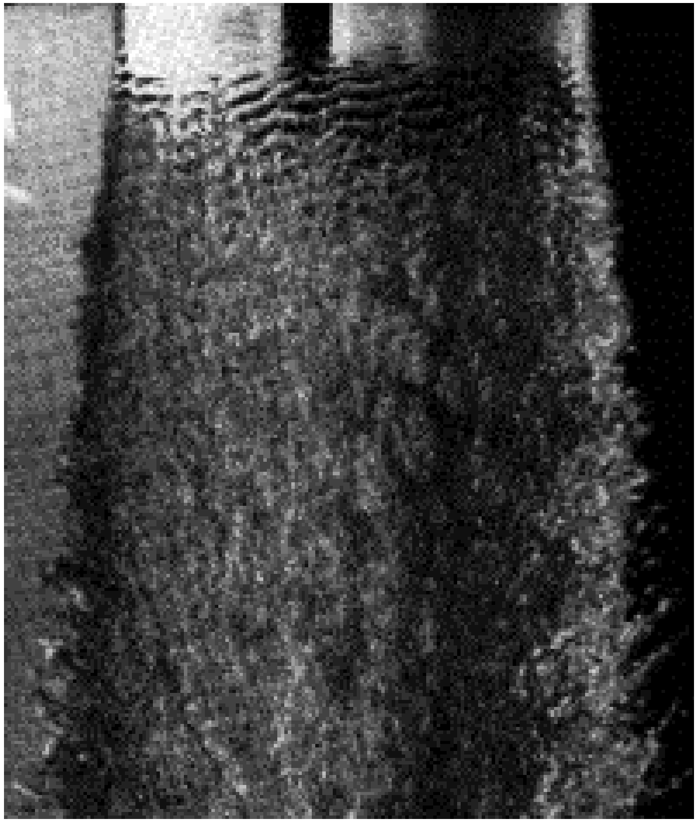

Taylor & Hoyt, 1983

High speed photograph of water jet close to nozzle exit (at top) in the second wind-induced breakup regime showing surface wave instability growth and breakup

Kelvin-Helmholtz Jet Breakup Model

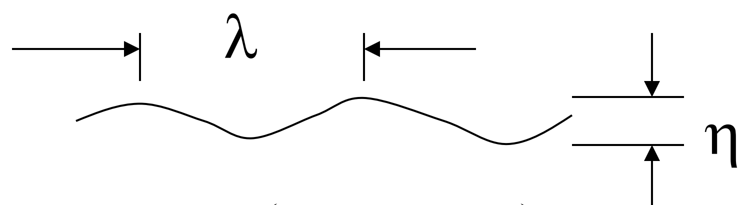

$$\eta = R\left(\eta_0 e^{ikz+\omega t}\right)$$

Linear Stability Theory:

Cylindrical liquid jet issuing from a circular orifice into a stationary, incompressible gas.

Relate growth rate, ω, of perturbation to wavelength $\lambda = 2\pi/k$

Reitz, 1982

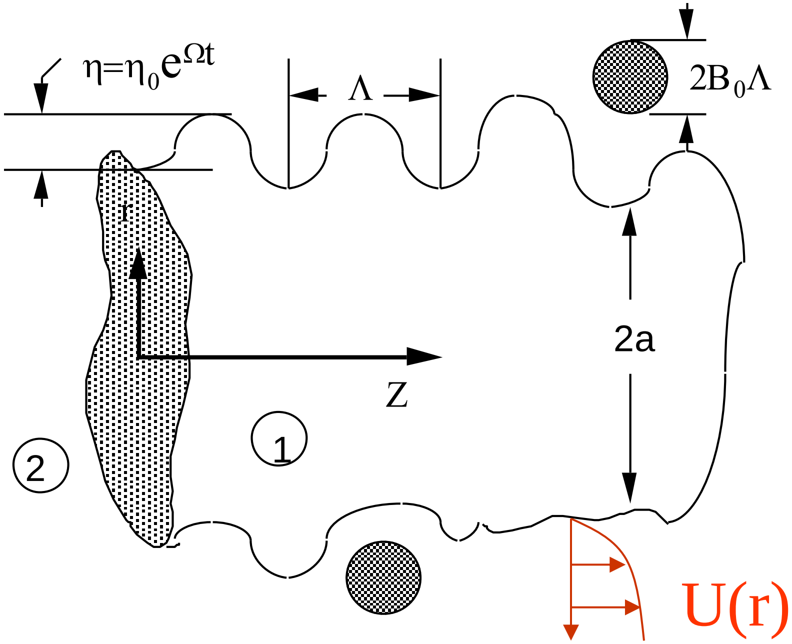

Linearized analysis

U = Jet velocity

Surface waves breakup on jet or "blob"

$$\eta = R\left(\eta_0 e^{ikz+\omega t}\right)$$

Equation of liquid surface: $r = a + \eta$,

Axisymmetric fluctuating pressure, axial velocity, and radial velocity for both liquid and gas phases.

Fluctuations described by continuity equation $\frac{\partial u_i}{\partial z} + \frac{1}{r}\frac{\partial}{\partial r}(r v_i) = 0$

plus linearized equations of motion for the liquid and the gas,

Axial: $$\frac{\partial u_i}{\partial t} + U_i(r)\frac{\partial u_i}{\partial z} + v_i\frac{dU_i}{dr} = -\frac{1}{\rho_i}\frac{\partial p_i}{\partial z} + \frac{\mu_i}{\rho_i}\left[\frac{\partial^2 u_i}{\partial z^2} + \frac{1}{r}\frac{\partial}{\partial r}\left(r\frac{\partial u_i}{\partial r}\right)\right]$$

Reitz, 1982

Analysis (Cont.)

Radial: $$\frac{\partial v_i}{\partial t} + U_i(r)\frac{\partial v_i}{\partial z} = -\frac{1}{\rho_i}\frac{\partial p_i}{\partial r} + \frac{\mu_i}{\rho_i}\left[\frac{\partial^2 v_i}{\partial z^2} + \frac{\partial}{\partial r}\left(\frac{1}{r}\frac{\partial r v_i}{\partial r}\right)\right]$$

Gas is assumed to be inviscid $U(r) = U$ - slip

With η <<a, the gas equations give the pressure at the interface $r = a$

$$p_2 = -\rho_2 (U - i\frac{\omega}{k})^2 k\eta \frac{K_0(ka)}{K_1(ka)}$$

Boundary conditions-

Kinematic, tangential and normal stress at the interface:

$$v_1 = \mathbf{w} = \frac{\partial \eta}{\partial t}, \qquad \frac{\partial u_1}{\partial r} = -\frac{\partial v_1}{\partial z}$$

$$-p_1 + 2\nu_1\rho_1\frac{\partial v_1}{\partial r} - \frac{\sigma}{a^2}(\eta + a^2\frac{\partial^2 \eta}{\partial z^2}) + p_2 = 0$$

Reitz, 1988

Dispersion relationship

$$\omega^2 + 2\nu_1 k^2 \omega \left[\frac{I_1'(ka)}{I_0(ka)} - \frac{2kl}{k^2+l^2}\frac{I_1(ka)}{I_0(ka)}\frac{I_1'(la)}{I_0(la)}\right] = \frac{\sigma k}{\rho_1 a^2}\left(1-k^2a^2\right)\left(\frac{l^2-k^2}{l^2+k^2}\right)\frac{I_1(ka)}{I_0(ka)}$$

$$+\frac{\rho_2}{\rho_1}(U - i\omega/k)^2 k^2 \left(\frac{l^2-k^2}{l^2+k^2}\right)\frac{I_1(ka)K_0(ka)}{I_0(ka)K_1(ka)}$$

Maximum wave growth rate characterizes fastest growing waves which are responsible for breakup
(as a function of Weber and Ohnesorge numbers)

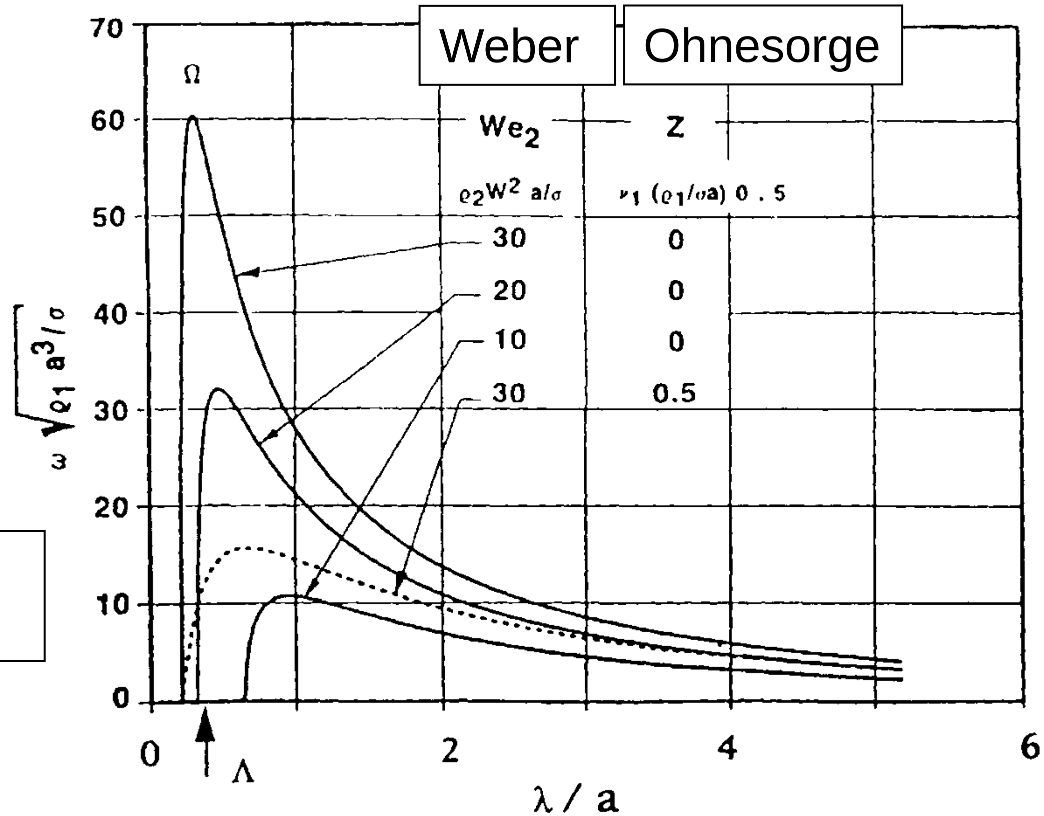

Maximum wave growth rate and length scale: Ω and Λ

Reitz, 1988

Curvefits of dispersion equation

$$\frac{\Lambda}{a} = 9.02\frac{\left(1 + 0.45 Z^{0.5}\right)\left(1 + 0.4T^{0.7}\right)}{\left(1 + 0.87 We_2^{1.67}\right)^{0.6}}$$

$$\Omega\left(\frac{\rho_1 a^3}{\sigma}\right)^{0.5} = \frac{0.34 + 0.38\, We_2^{1.5}}{(1 + Z)\left(1 + 1.4T^{0.6}\right)}$$

where $Z=\frac{We_1^{0.5}}{Re_1}$; $T=ZWe_2^{0.5}$; $We_1=\frac{\rho_1 U^2 a}{\sigma}$; $We_2=\frac{\rho_2 U^2 a}{\sigma}$; $Re_1=\frac{Ua}{\nu_1}$

Maximum growth rate increases and wavelength decreases with We

Increased viscosity reduces growth rate and increases wave length

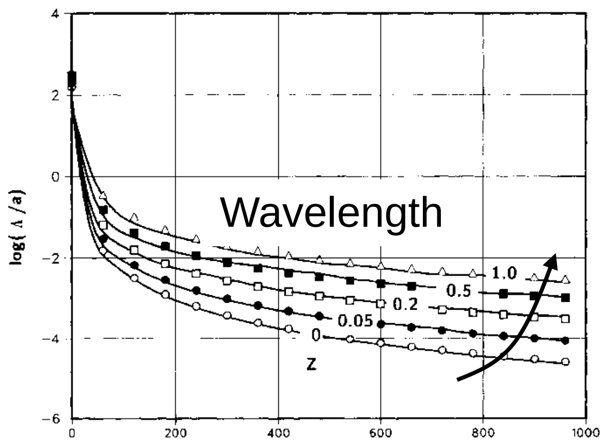

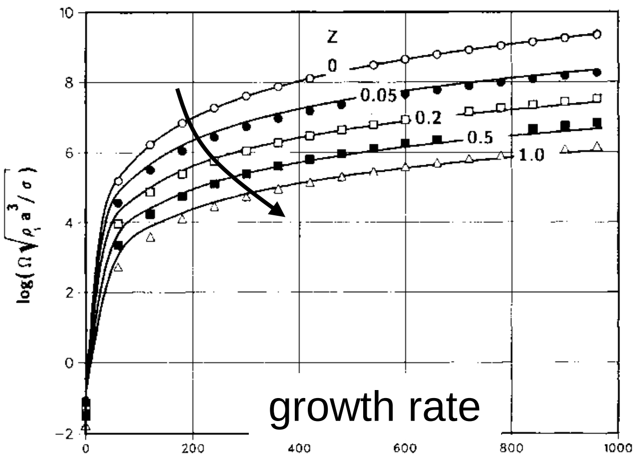

Reitz, 1988

"Wave" atomization model

Drop size: $r = B\Lambda$

Breakup time: $\tau \sim \Omega^{-1}$

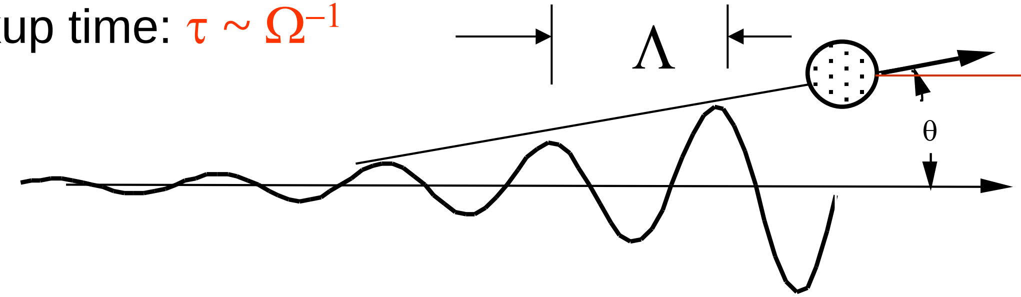

Spray angle prediction:

$$Tan\ \theta = \frac{v}{U} = \frac{1}{A} 4\pi \left(\frac{\rho_2}{\rho_1}\right)^{1/2} f(T)$$

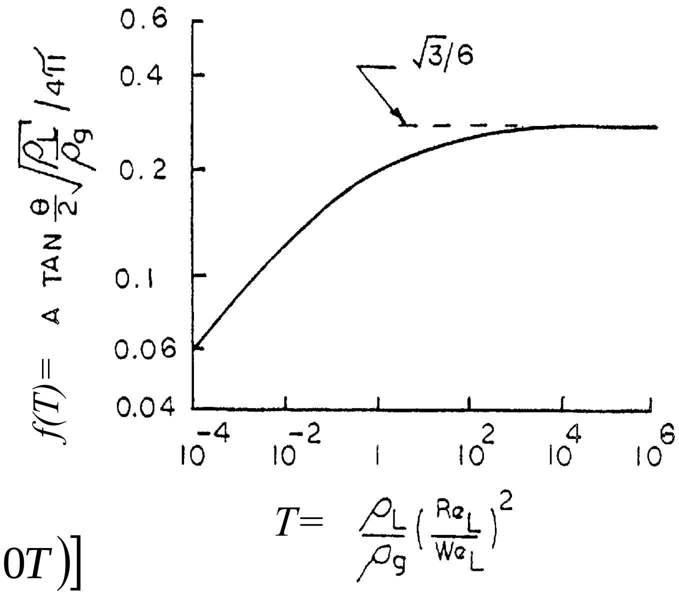

Breakup length of the core (Taylor, 1940):

$$L = C\, a \sqrt{\frac{\rho_1}{\rho_2}} / f(T) \quad \text{where} \quad f(T) = \frac{\sqrt{3}}{6}\left[1 - \exp(-10T)\right]$$

Gao, 2010

X-ray Phase-contrast imaging of high-pressure sprays

ANL Synchrotron-Based Ultrafast (150 ps) Single-Shot images

Surface instability waves produce ligaments
Breakup sensitive to injection pressure, fuel properties

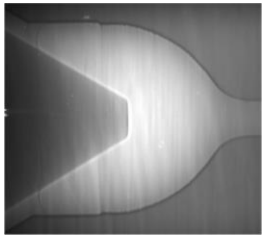

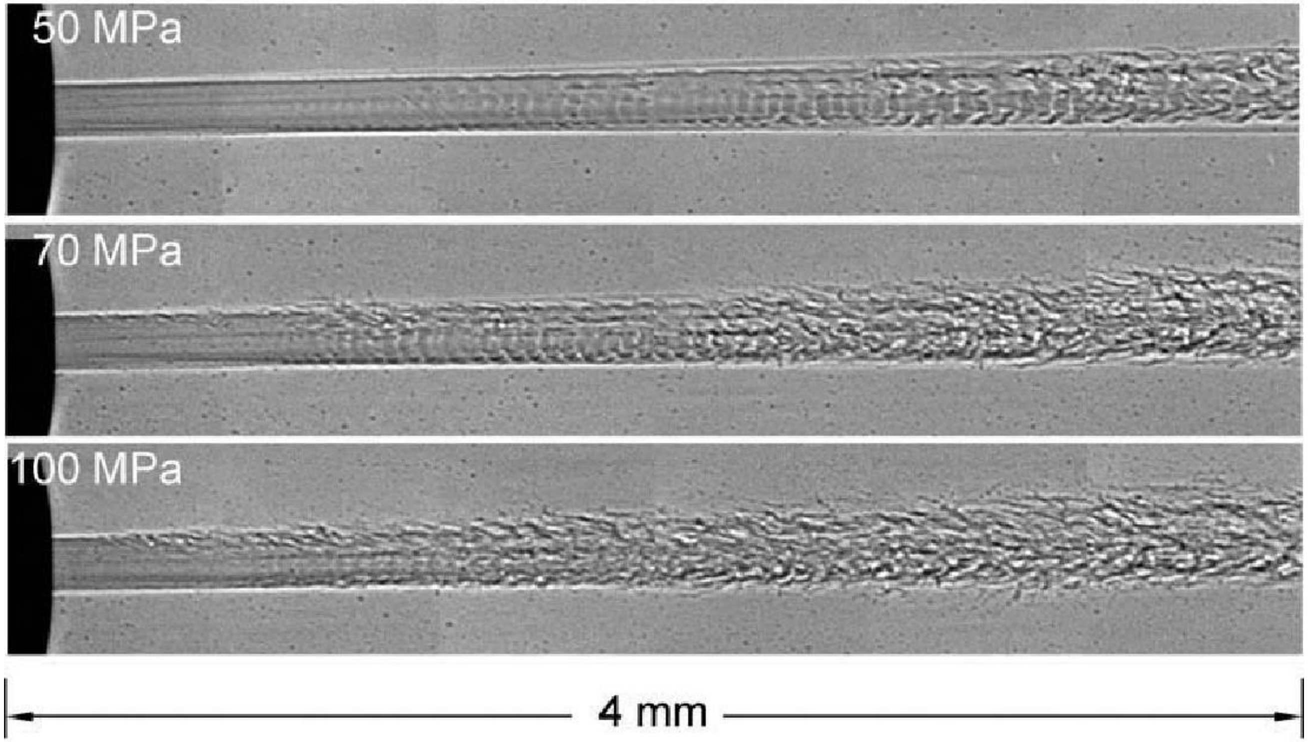

(Hydroground nozzle, biodiesel, 1 ms injection duration in quasi-steady state)

Beale, 1999
Rutland, 2011
Deshpande, 2013

ERC spray modeling

LDEF - RANS Approach - Reitz

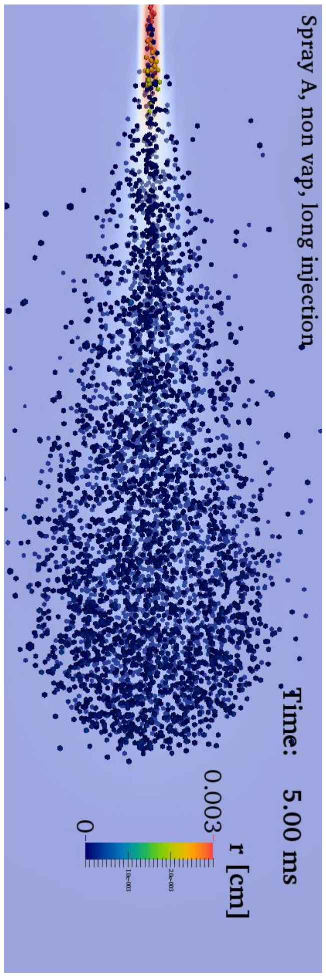

LDEF – LES Approach - Rutland

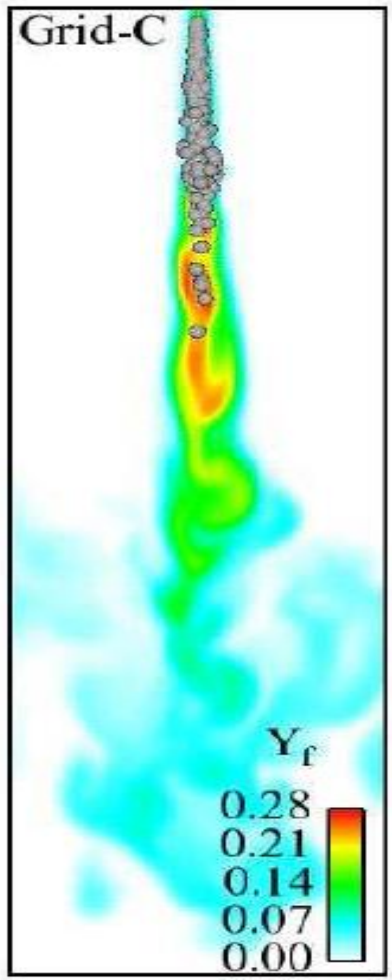

Pure Eulerian DNS Approach - Trujillo

Track liquid-gas interface with VOF method

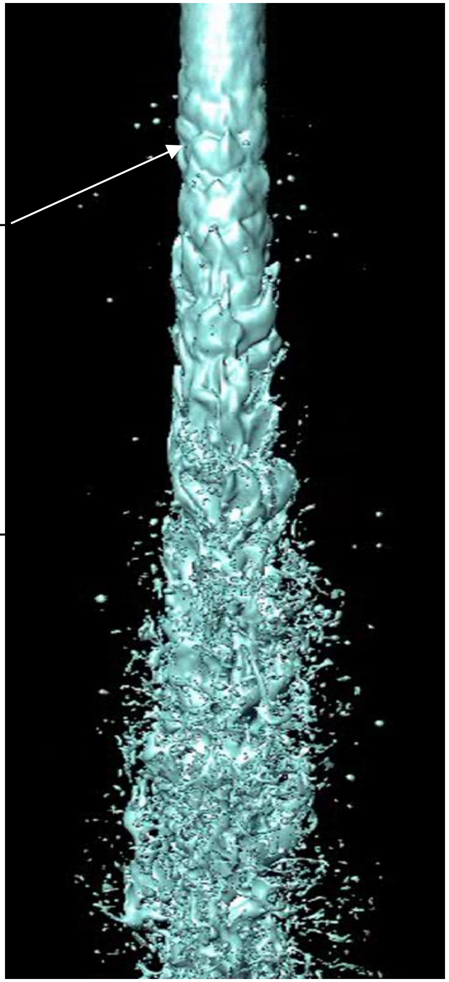

ELSA model Modeling liquid-gas surface area density [1-5]

- $\tilde{\Sigma}$: Liquid-Air surface area per unit mass:

$$\frac{\partial \bar{\rho}\tilde{\Sigma}}{\partial t} + \nabla \cdot \left(\bar{\rho}\tilde{\Sigma}\tilde{\mathbf{u}} \right) = \nabla \cdot \left[\frac{\mu_t}{Sc_\Sigma} \left(\nabla \tilde{\Sigma} \right) \right] + a\bar{\rho}\tilde{\Sigma}\left(1 - \frac{\tilde{\Sigma}}{\tilde{\Sigma}_{eq}} \right)$$

$$\begin{cases} r_{eq} = C \dfrac{\sigma^{3/5} l_t^{2/5}}{\tilde{k}^{3/5}} \dfrac{\left(\bar{\rho}\tilde{Y} \right)^{2/15}}{\rho_L^{11/15}} \\ We_{eq} = \dfrac{\rho_l \left(\Delta v \right)^2 r_{eq}}{\sigma} = C \sim O(1) \end{cases}$$

Liquid-Gas Surface Area Density [5]: Comparing Modeling and DNS

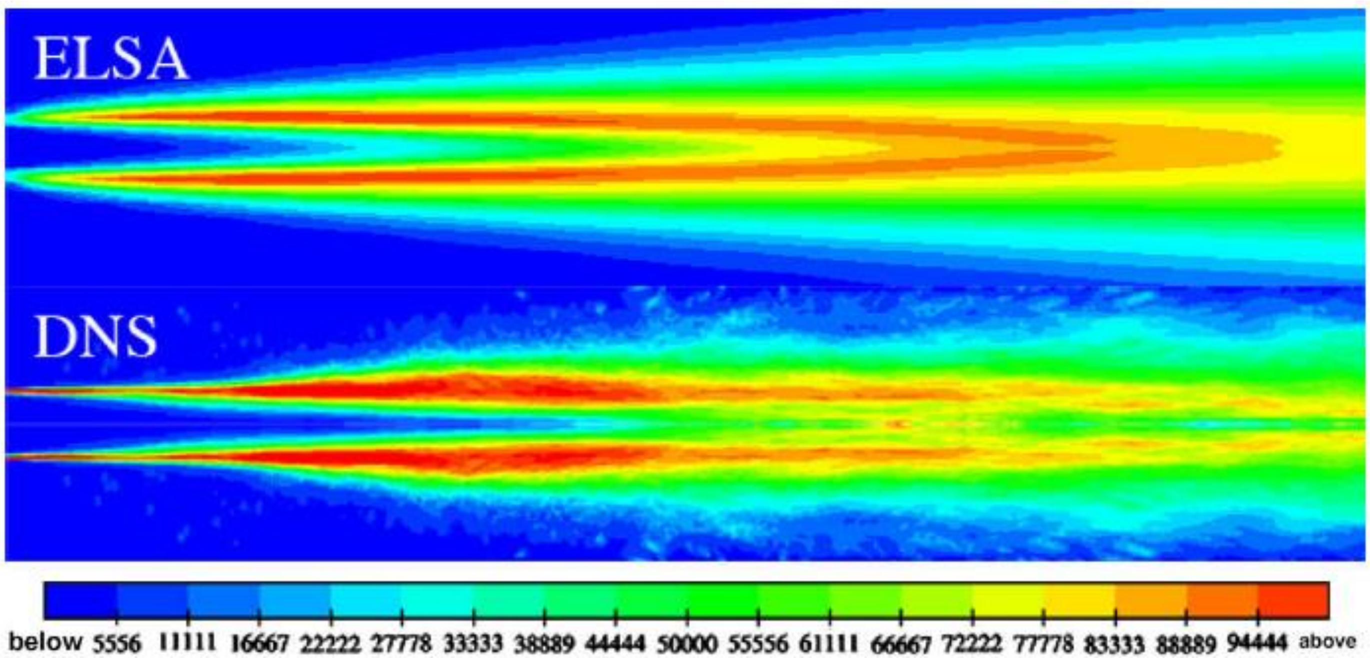

ELSA model - Modeling liquid-gas surface area density [1-5]

- Eulerian-Lagrangian transition in the dispersed spray region

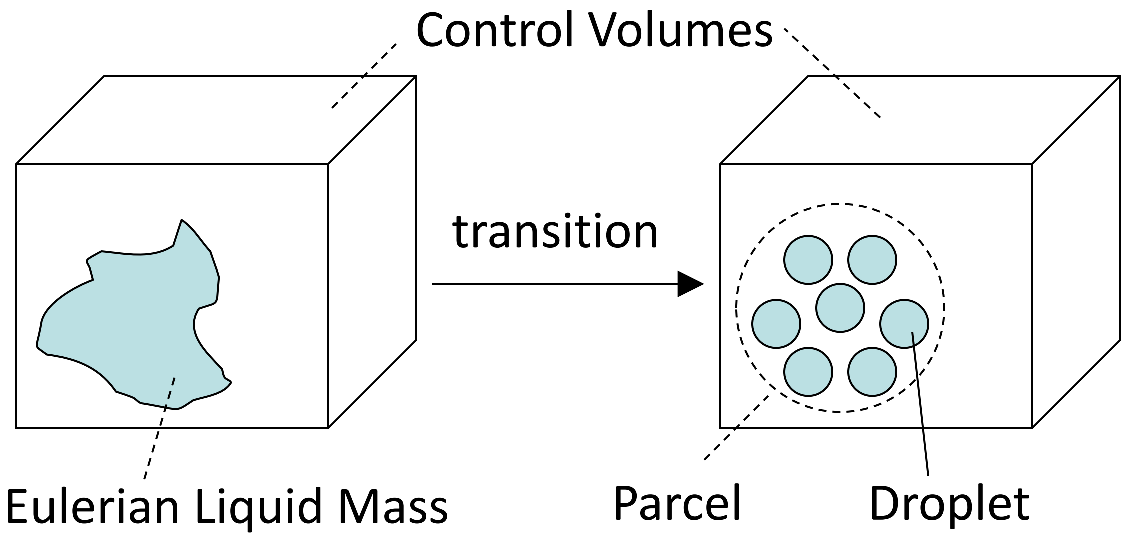

Droplet size: based on the local surface area density

Droplet number: based on droplet size, as well as the liquid mass inside the cell

- Advantages:

Naturally works with RANS and does not require expensive mesh resolution.

- Criterion for transition:

(A) Liquid volume fraction is less than a threshold value;
(B) Liquid mass in the cell is larger than a threshold value

Wang, 2013

ELSA model Modeling liquid-gas surface area density [1-5]

- Axi-Symmetric Round Nozzle
- L=1.025 mm, D = 139 µm
- Injection Pressure: 400 bar, Chamber Pressure: 20 bar
- Sharp corner at inlet, rounded corner at inlet with r/R=1

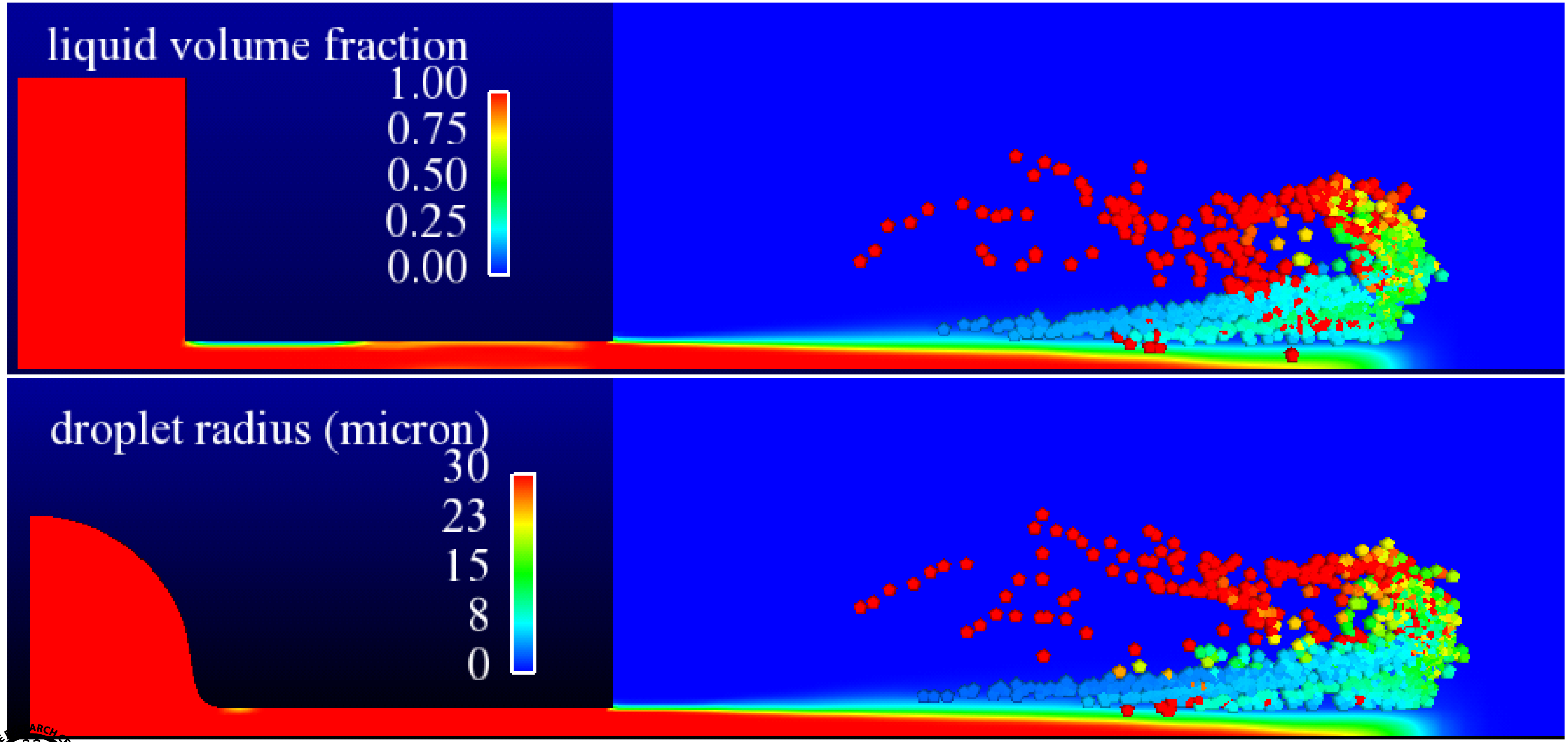

Liu, 1997

Drop breakup

Mechanisms of drop breakup at high velocities poorly understood - Conflicting theories

Bag, 'Shear' and 'Catastrophic' breakup regimes

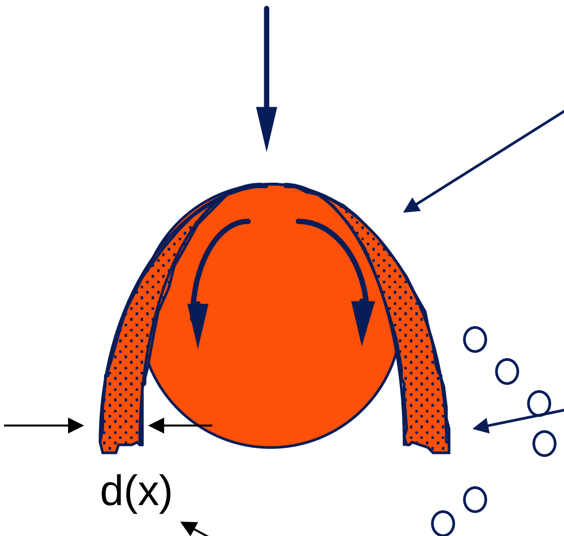

Breakup due to capillary surface waves

Hinze Chem Eng (1955) and
Engel Nat. Bureau Stds (1958)

Boundary Layer Stripping due to Shear at the interface

Ranger and Nicolls AIAA J. (1969)
Reinecke and Waldman AVCO Rep (1970)

Delplanque & Sirignano Atom Sprays (1994)

Stretching and thinning – drop distortion - Liu and Reitz IJMF (1997)

Liu, 1993

Low velocity drop breakup

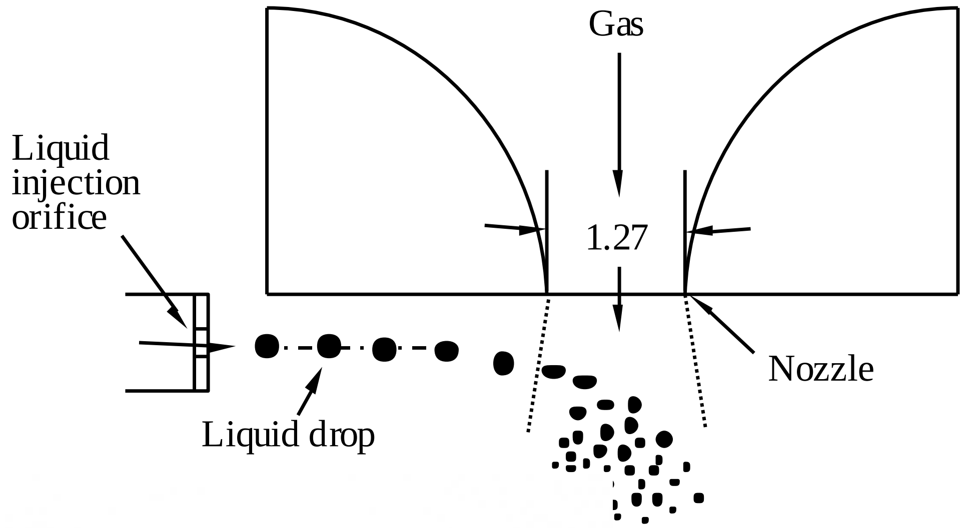

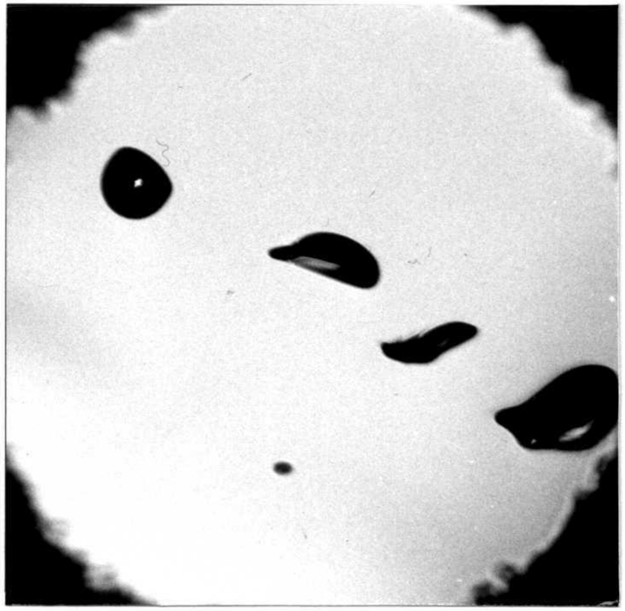

(a) bag breakup (We=78)

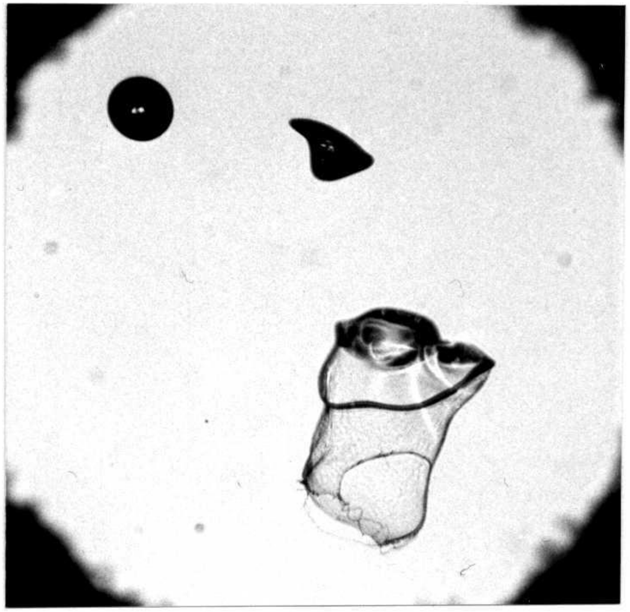

(b) bag breakup (We=98)

Hwang, 1996

High speed drop breakup mechanism

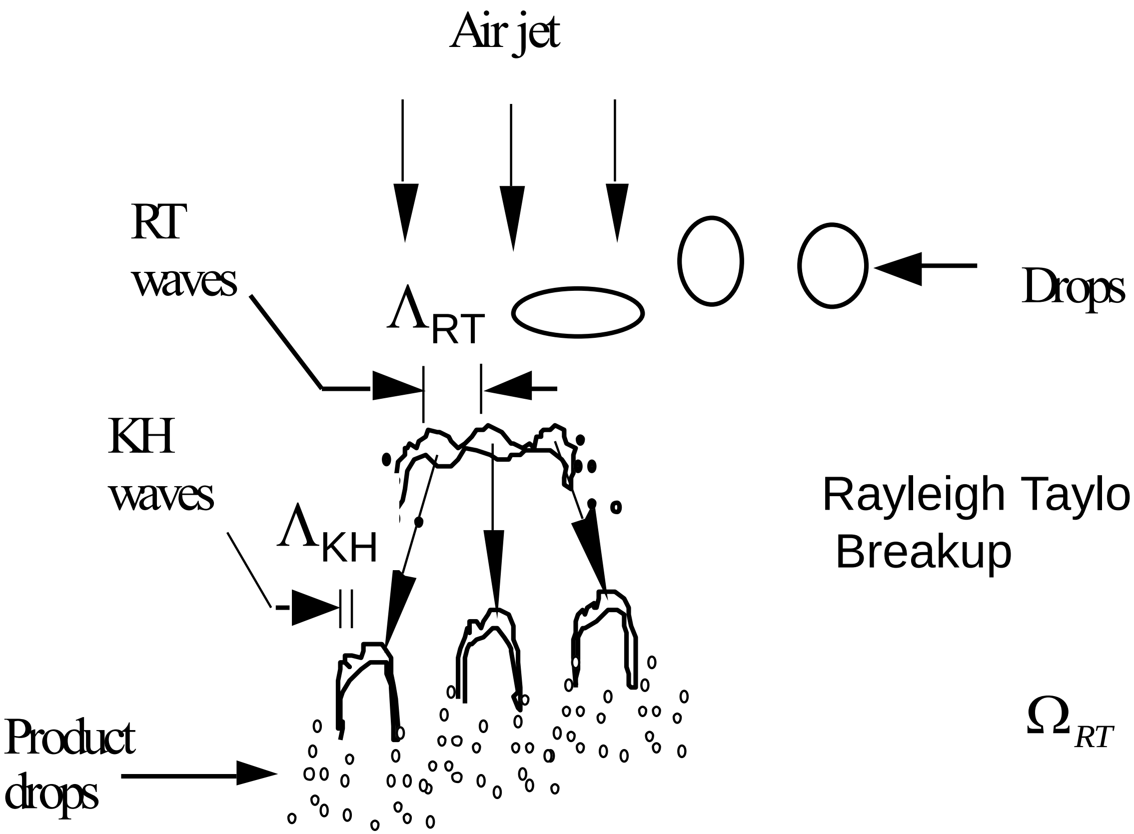

Double pulse images

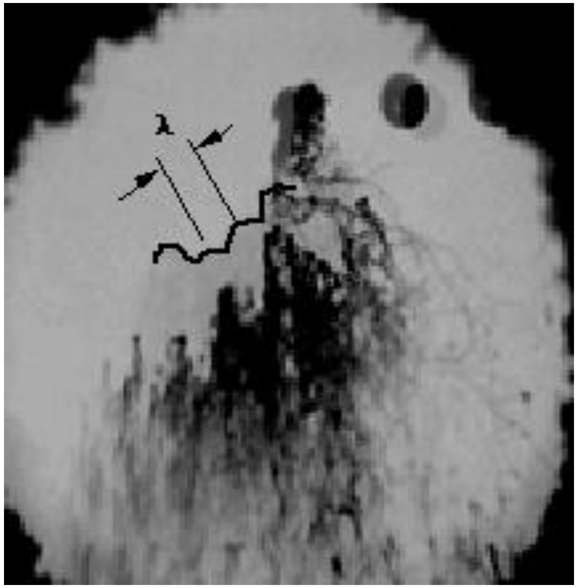

Rayleigh Taylor Breakup

$$\Omega_{RT} = \sqrt{\frac{2}{3\sqrt{\sigma}} \frac{\left[-g_t\left(\rho_l - \rho_g\right)\right]^{3/2}}{\rho_l + \rho_g}}$$

g_t = acceleration

$$\Lambda_{RT} = \sqrt{\frac{-g_t\left(\rho_l - \rho_g\right)}{3\sigma}}$$

Lee, 2001

Drop breakup regimes

Breakup stages	Deformation or breakup regimes	Breakup process	Weber number	References
First breakup stage	(1) Deformation and flattening	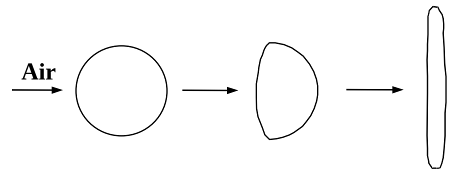	We < 12	
Second breakup stage	(b) Bag breakup	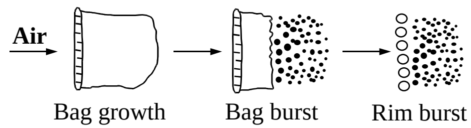	12 ≤ We ≤ 100 (including the Bag-and-Stamen breakup)	Pilch and Erdman
	(c) Shear breakup	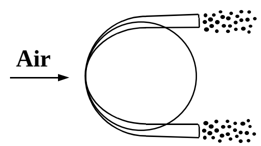	We < 80	Ranger and Nicolls 1969
	(d) Stretching and thinning breakup	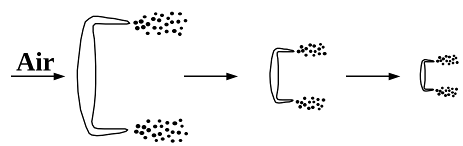	100 ≤ We ≤ 350	Liu and Reitz 1997
	(e) Catastrophic breakup	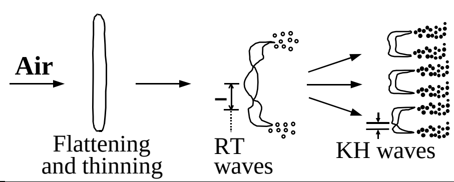	350 ≤ We	Hwang et al. 1996

O'Rourke, 1981

Drop collision modeling

Collision frequency

$$\nu_{12} = N_2 \pi (r_1 + r_2)^2 E_{12} |\mathbf{v}_1 - \mathbf{v}_2| / Vol$$

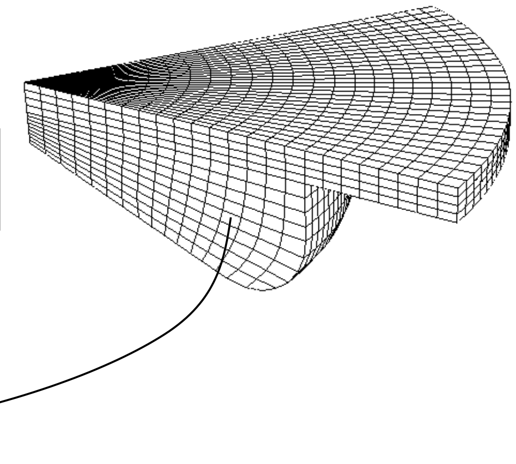

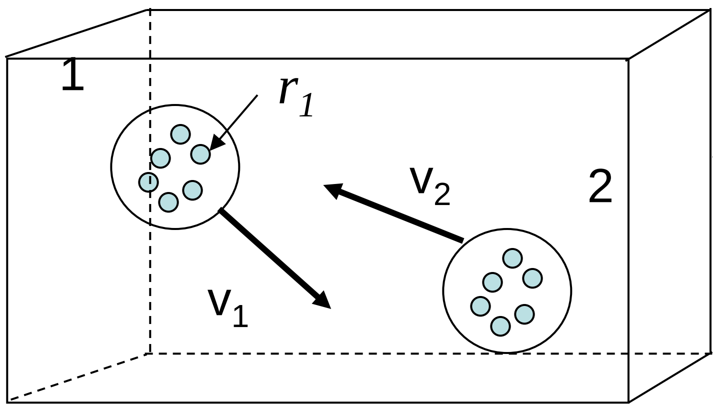

Number of collisions from Poisson process

$$p(n) = e^{-\nu_{12}\Delta t} (\nu_{12} \Delta t)^n / n!$$

$0 < p < 1$ random number

Collision efficiency

$$E_{12} = \left(\frac{K}{K + 1/2} \right)^2 \sim 1$$

$$K = \frac{2}{9} \frac{\rho_l |\mathbf{v}_1 - \mathbf{v}_2| r_2^2}{\mu_g r_1}$$

Munnannur, 2007
Georjon, 1999

Drop collision and coalescence

1. Reflexive vs. surface energy
2. Kinetic energy of unaffected part vs. surface energy
3. Drops cannot expel trapped gas film (bounce apart)
4. Drops form combined mass (coalesce)

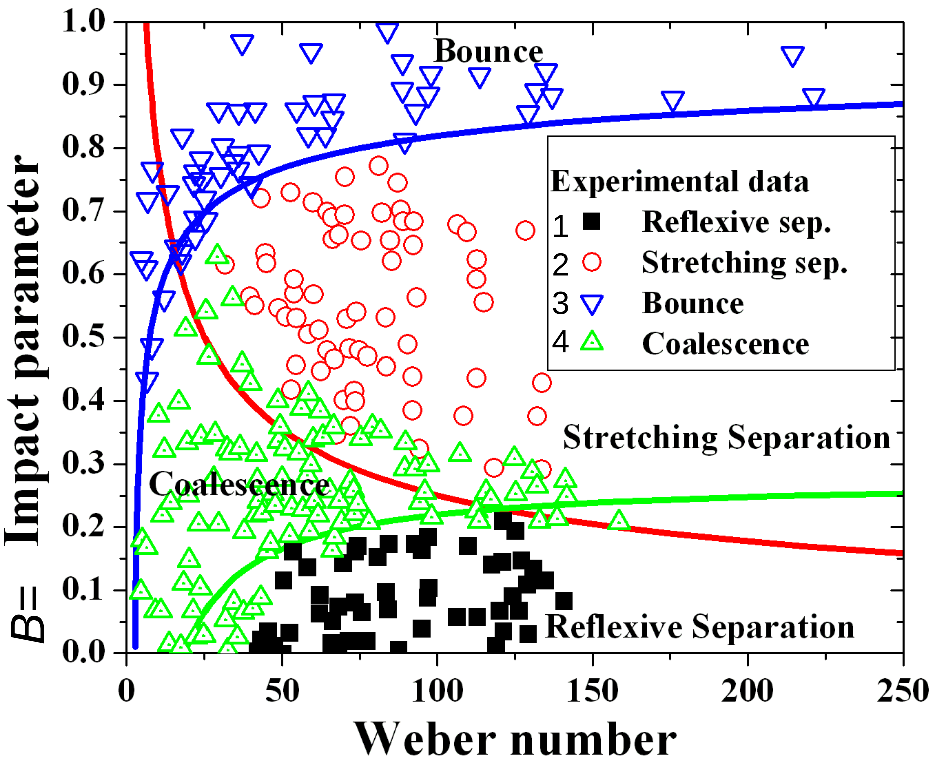

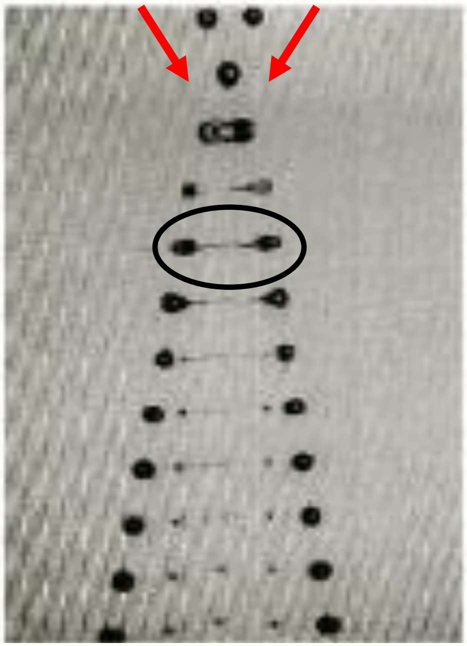

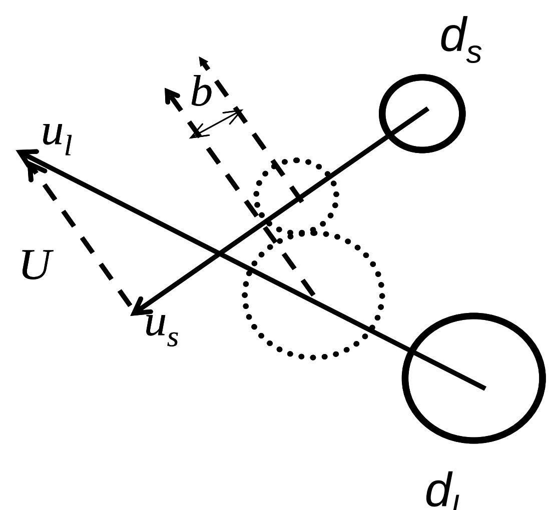

$$We = \frac{\rho_L U^2 d_s}{\sigma}, \quad B = \frac{2b}{(d_s + d_l)}, \quad \Delta = \frac{d_s}{d_l}$$

Ashgriz, 1990

Drop coalescence

Grazing-coalescence boundary

Drops fly apart if rotational energy of colliding pair exceeds surface energy of combined pair

$$B = \sqrt{\frac{12}{5\,We}}\,\frac{\left(1+\Delta^3\right)^{11/6}}{\left(1+\Delta\right)\Delta^3}\left[1+\Delta^2-\left(1+\Delta^3\right)^{2/3}\right]^{1/2}$$

$0 < B < 1$
random number

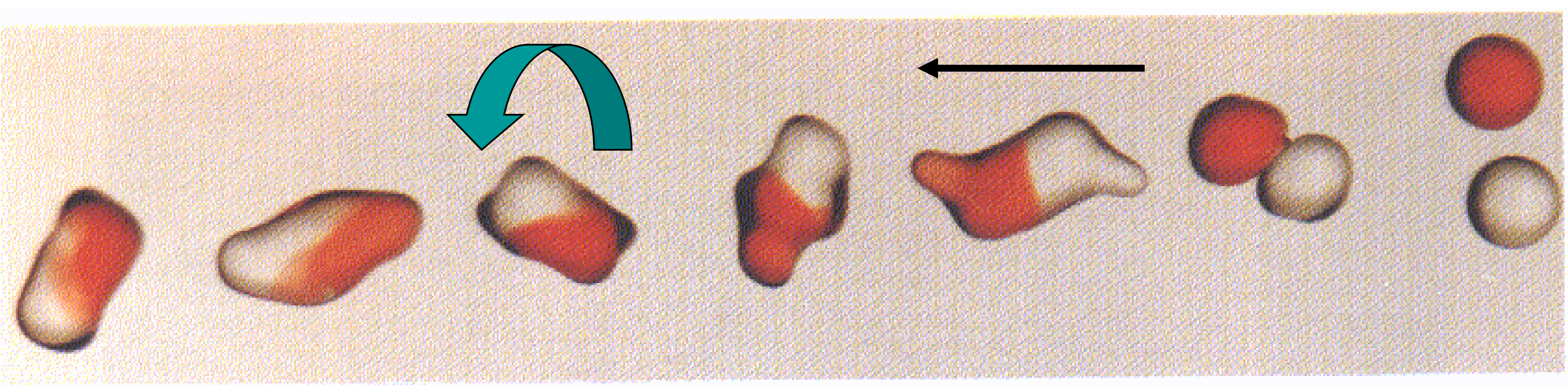

FIGURE 15. Coalescence collision at $\Delta = 1$, $We = 10$, and $B = 0.5$.

Ashgriz, 1990

Grazing - stretching separation

Energy and angular momentum conservation:

Grazing – drops move in same direction but at reduced velocity
Coalescence – mass average properties of colliding drops

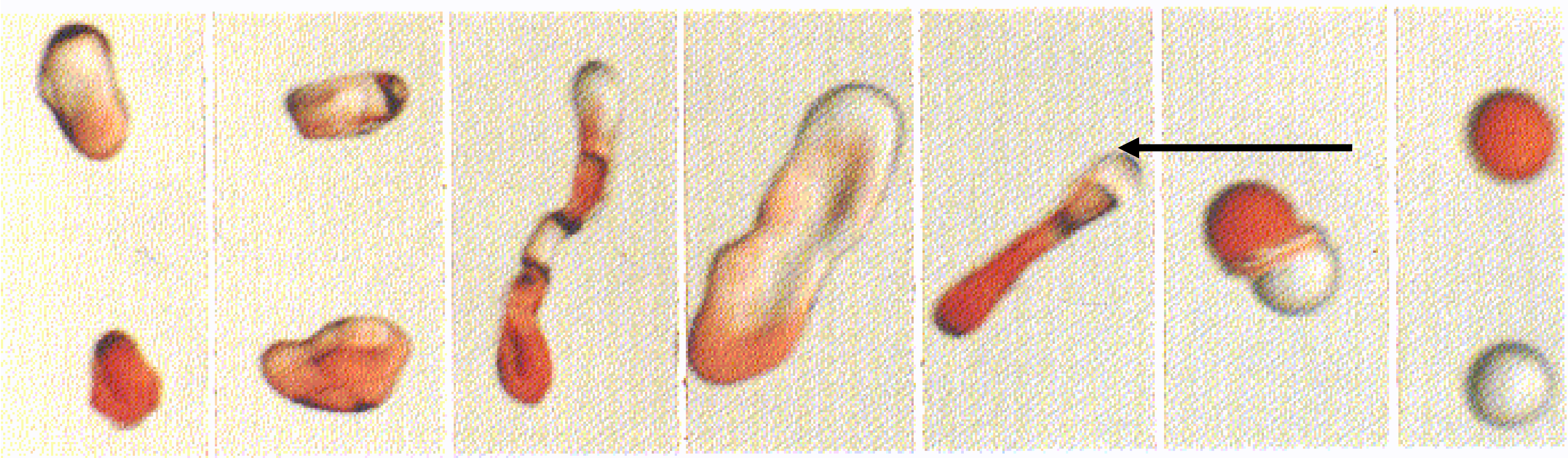

FIGURE 12. Stretching separation at $\Delta = 1$, $We = 53$, and $B = 0.38$.

Ashgriz, 1990

Reflexive separation

Tennison, 1998

$$\frac{2\,We}{\Delta\left(1+\Delta^3\right)^2}\left(\Delta^6\,\eta_1+\eta_2\right)+3\left[4\left(1+\Delta^2\right)-7\left(1+\Delta^3\right)^{2/3}\right]\geq 0$$

$$\eta_1 = 2\left(1-\xi\right)^2\left(1-\xi^2\right)^{1/2}-1$$

$$\eta_2 = 2\left(\Delta-\xi\right)^2\left(\Delta^2-\xi^2\right)^{1/2}-\Delta^3$$

with $\xi = B\,(1+\Delta)/2$

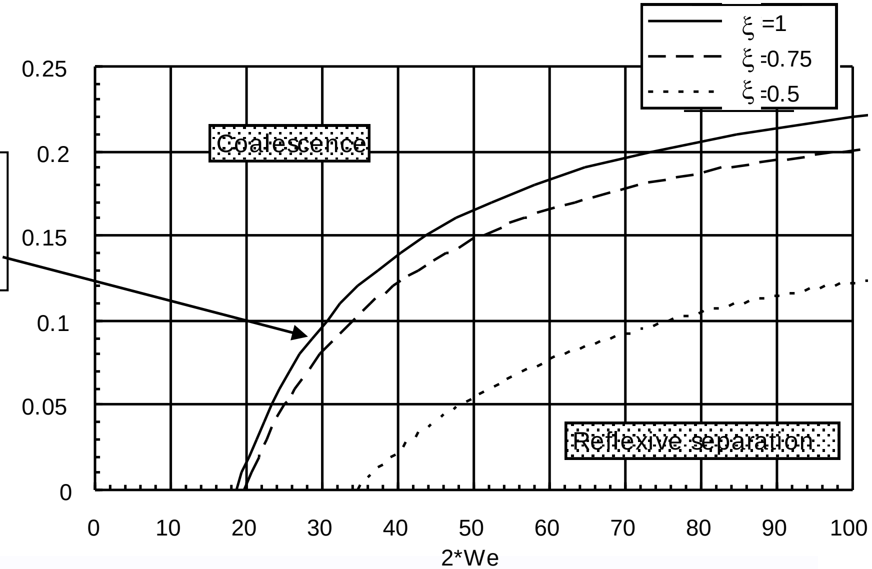

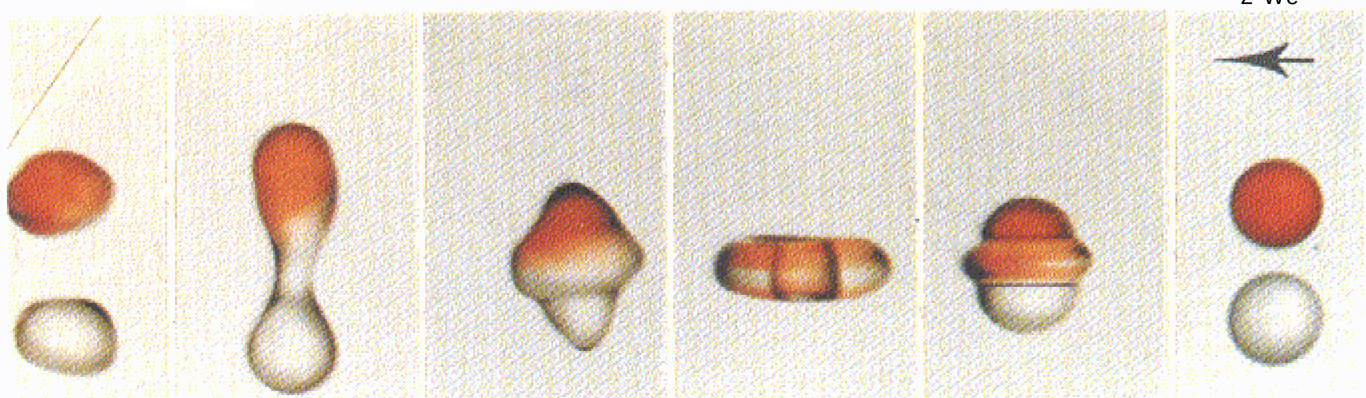

FIGURE 5. Reflexive separation with no satellite for Δ = 1, We = 23, and B = 0.05.

Summary

The Lagrangian Drop/Eulerian Fluid (LDEF) Discrete Drop model is the work-horse approach in commercial codes for simulating 2-phase flows.

Detailed models are available for use in engine CFD models to describe the effects of injector nozzle flow, and liquid and gas properties on spray formation and drop breakup physics.

Due to the importance of sprays in applications, research is still needed. Recent experimental and modeling work can be accessed through ILASS and ICLASS conference papers and the Atomization and Sprays journal.

Significant progress is being made using LES/DNS spray modeling with high resolution experimental diagnostics to validate engine CFD spray models.

Ballistic imaging: Linne, 2009; **X-Ray imaging:** Liu SAE paper 2010-01-0877

LES: Villiers & Gosman, LES Primary Diesel Spray Atomization, SAE 2004-01-0100

DNS: Near field spray modeling (Trujillo - ERC)

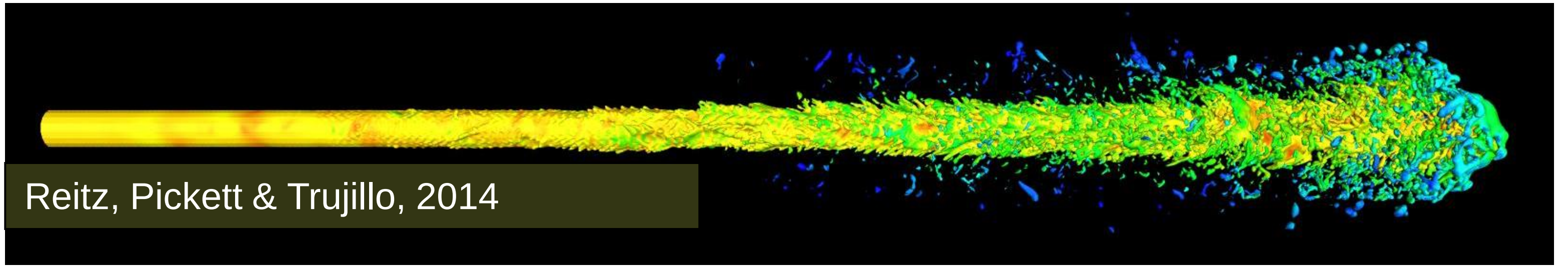

Reitz, Pickett & Trujillo, 2014